Article

Developmental Cell

Transcription factor induction of vascular blood stem cell niches *in vivo*

Graphical abstract

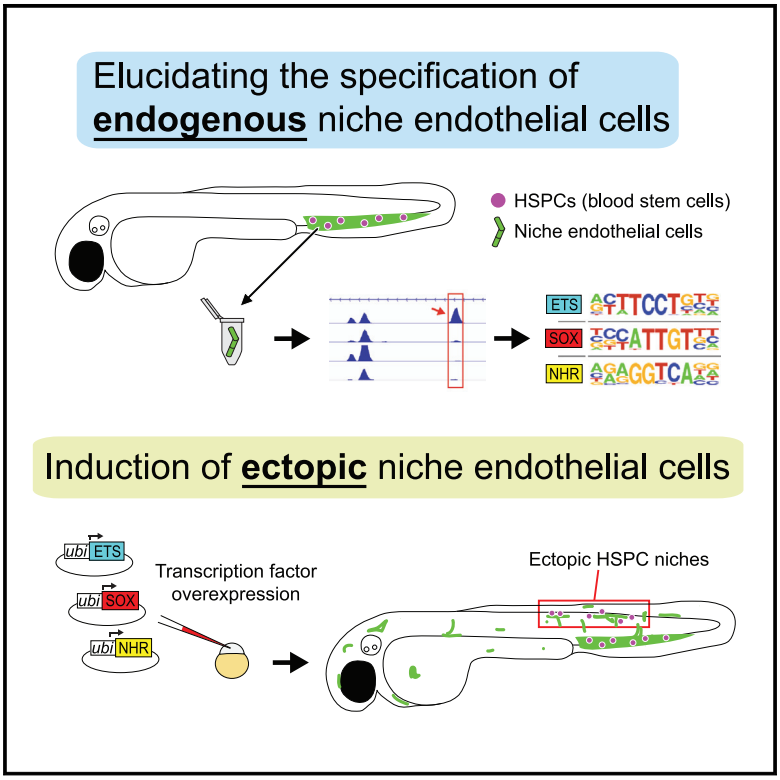

Highlights

- Multi-dimensional expression analysis identifies endothelial signatures for HSPC niches
- Study defines *cis*-regulatory landscape underlying niche endothelial identity
- 3-factor combination induces ectopic niche endothelial cells that support HSPCs

Authors

Elliott J. Hagedorn, Julie R. Perlin, Rebecca J. Freeman, ..., Shahin Rafii, J. Philipp Junker, Leonard I. Zon

Correspondence

zon@enders.tch.harvard.edu

In brief

Hagedorn et al. use a combination of genomic techniques to elucidate an endothelial signature unique to blood stem cell niches. They define the underlying *cis*-regulatory landscape and a transcription factor combination that can reprogram embryonic cells into niche endothelial cells that can recruit and support blood stem cells.

Hagedorn et al., 2023, Developmental Cell *58*, 1037–1051
June 19, 2023 © 2023 The Authors. Published by Elsevier Inc.
https://doi.org/10.1016/j.devcel.2023.04.007

CellPress

Developmental Cell

CellPress
OPEN ACCESS

Article

Transcription factor induction of vascular blood stem cell niches *in vivo*

Elliott J. Hagedorn,[1,2,8] Julie R. Perlin,[1] Rebecca J. Freeman,[1] Samuel J. Wattrus,[1] Tianxiao Han,[1] Clara Mao,[1] Ji Wook Kim,[1] Inés Fernández-Maestre,[1] Madeleine L. Daily,[1] Christopher D'Amato,[1] Michael J. Fairchild,[1] Raquel Riquelme,[1] Brian Li,[1] Dana A.V.E. Ragoonanan,[2] Khaliun Enkhbayar,[2] Emily L. Henault,[2] Helen G. Wang,[2] Shelby E. Redfield,[1] Samantha H. Collins,[1] Asher Lichtig,[1] Song Yang,[1] Yi Zhou,[1] Balvir Kunar,[3] Jesus Maria Gomez-Salinero,[3] Thanh T. Dinh,[4] Junliang Pan,[4] Karoline Holler,[5] Henry A. Feldman,[6] Eugene C. Butcher,[4] Alexander van Oudenaarden,[7] Shahin Rafii,[3] J. Philipp Junker,[5] and Leonard I. Zon[1,9,*]

[1]Stem Cell Program and Division of Hematology/Oncology, Boston Children's Hospital and Dana Farber Cancer Institute, Howard Hughes Medical Institute, Harvard Medical School, Harvard Stem Cell Institute, Stem Cell and Regenerative Biology Department, Harvard University, Boston, MA, USA

[2]Section of Hematology and Medical Oncology and Center for Regenerative Medicine, Boston University School of Medicine and Boston Medical Center, Boston, MA, USA

[3]Ansary Stem Cell Institute, Division of Regenerative Medicine, Department of Medicine, Weill Cornell Medicine, New York, NY, USA

[4]Veterans Affairs Palo Alto Health Care System, The Palo Alto Veterans Institute for Research and the Department of Pathology, Stanford University, Stanford, CA, USA

[5]Berlin Institute for Medical Systems Biology, Max Delbruck Center for Molecular Medicine, Berlin, Germany

[6]Institutional Centers for Clinical and Translational Research, Boston Children's Hospital, Boston, MA, USA

[7]Hubrecht Institute, Royal Netherlands Academy of Arts and Sciences and University Medical Center Utrecht, Utrecht, the Netherlands

[8]Present address: Section of Hematology and Medical Oncology and Center for Regenerative Medicine, Boston University School of Medicine and Boston Medical Center, Boston, MA, USA

[9]Lead contact

*Correspondence: zon@enders.tch.harvard.edu

https://doi.org/10.1016/j.devcel.2023.04.007

SUMMARY

The hematopoietic niche is a supportive microenvironment composed of distinct cell types, including specialized vascular endothelial cells that directly interact with hematopoietic stem and progenitor cells (HSPCs). The molecular factors that specify niche endothelial cells and orchestrate HSPC homeostasis remain largely unknown. Using multi-dimensional gene expression and chromatin accessibility analyses in zebrafish, we define a conserved gene expression signature and *cis*-regulatory landscape that are unique to sinusoidal endothelial cells in the HSPC niche. Using enhancer mutagenesis and transcription factor overexpression, we elucidate a transcriptional code that involves members of the Ets, Sox, and nuclear hormone receptor families and is sufficient to induce ectopic niche endothelial cells that associate with mesenchymal stromal cells and support the recruitment, maintenance, and division of HSPCs *in vivo*. These studies set forth an approach for generating synthetic HSPC niches, *in vitro* or *in vivo*, and for effective therapies to modulate the endogenous niche.

INTRODUCTION

Hematopoietic stem and progenitor cells (HSPCs) are a rare population of cells capable of reconstituting the entire blood system.[1] In the bone marrow, multiple cell types are thought to contribute to the HSPC niche, with endothelial cells (ECs) being a primary component.[2–7] Distinct endothelial subtypes differentially regulate HSPCs: arterial ECs (AECs) promote HSPC quiescence, whereas sinusoidal ECs (SECs) support HSPC differentiation and mobilization.[8–10] Specialized bone marrow ECs play a critical role in niche reconstruction and hematopoietic recovery after myelosuppression,[11,12] and ECs support HSPCs outside the bone marrow during development and stress-induced hematopoiesis.[13]

HSPCs are born in the aorta-gonad-mesonephros region and then migrate to a transient fetal niche, the liver in mammals, or a venous plexus in the tail of fish called the caudal hematopoietic tissue (CHT).[1,14] HSPCs expand in these sites for several days before migrating to the adult niche, the bone marrow in mammals, or the kidney marrow in fish. The CHT is composed of low-flow venous SECs.[14–19] As HSPCs lodge in the CHT, ECs reorganize to form supportive pockets, which together with perivascular stromal cells form a niche.[17] Specific signaling molecules, adhesion proteins, and transcription factors are implicated in mediating cross-talk and physical interaction between stem cells and ECs in the niche.[2,20–26] Understanding the transcriptional regulation of these molecules could guide strategies

This is an open access article under the CC BY license (http://creativecommons.org/licenses/by/4.0/).

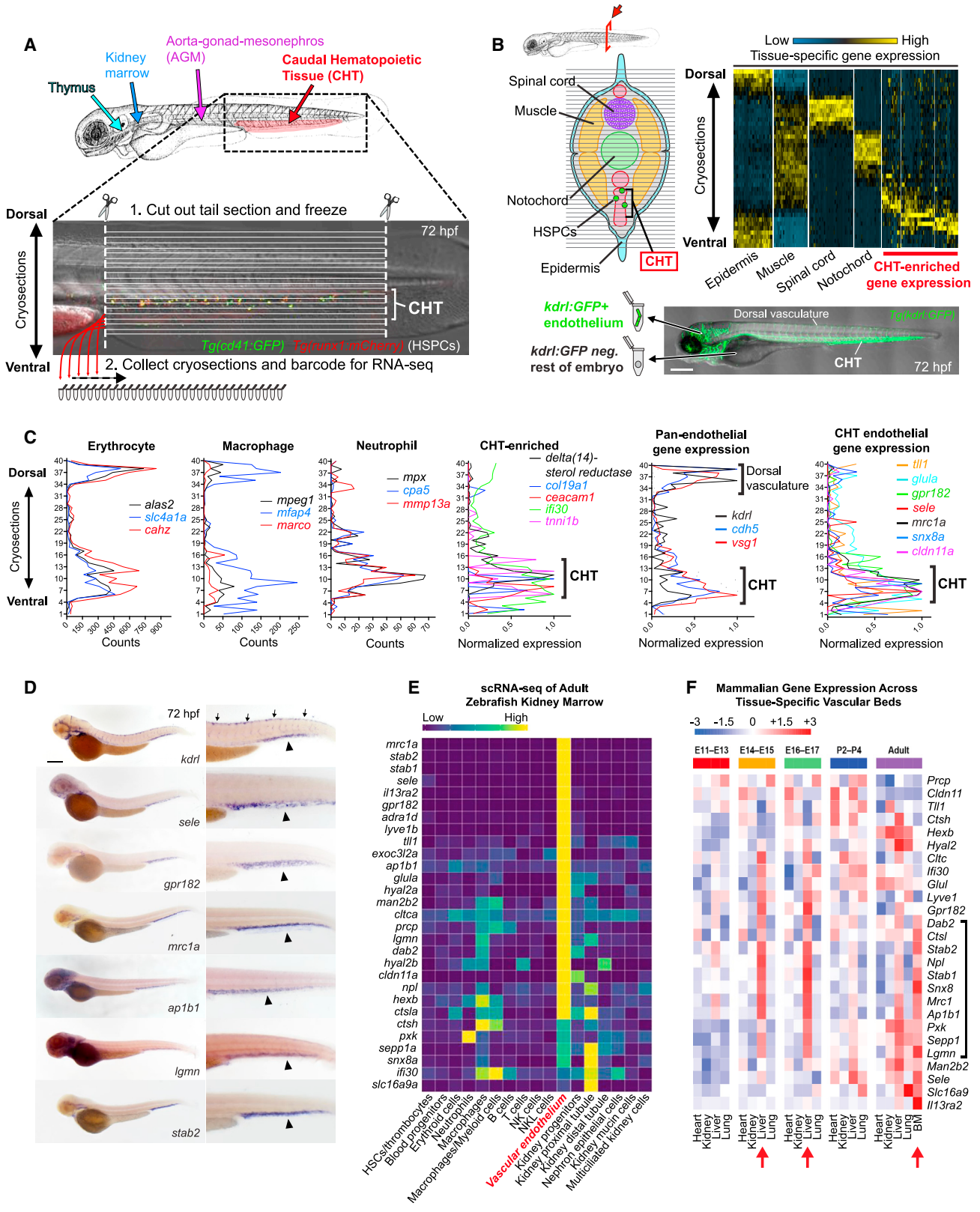

Figure 1. An endothelial gene expression signature unique to HSPC niches

(A) Schematic diagram illustrates the hematopoietic tissues of the zebrafish embryo (top) and the sectioning strategy used to perform RNA tomography (tomo-seq) on the CHT (bottom; double transgenic embryo carrying the HSPC markers *cd41:GFP* and *runx1:mCherry* is shown).

(legend continued on next page)

CellPress
OPEN ACCESS

to improve the efficacy and availability of bone marrow transplantation.

RESULTS

An endothelial gene expression signature unique to HSPC niches

To investigate gene expression in the CHT, we performed RNA tomography (tomo-seq)[27] on the zebrafish tail at 72 hours post-fertilization (hpf), sectioning along the dorsal-ventral axis (Figure 1A). This revealed clusters of gene expression corresponding to specific tissues within the tail, including the spinal cord, muscle, notochord, epidermis, and distinct hematopoietic populations (Figures 1B and 1C). From this dataset, we found 144 genes enriched in the CHT (Figure 1B; Table S1). Using a combination of EC-specific RNA-seq, published myeloid RNA-seq datasets,[28] and whole-mount *in situ* hybridization (WISH), we identified 29/144 genes that were selectively expressed by ECs in the CHT (Figures 1B, 1D, and S1A; Table S2). Using published whole kidney and EC-specific single-cell RNA-seq data generated in this study, we found that 23 of these 29 genes were expressed by venous SECs in the adult kidney (Figures 1E and S1B), a population associated with hematopoiesis in fish.[29] The orthologs for 21/29 CHT EC genes were enriched in the ECs of mammalian hematopoietic organs[30]—the fetal liver and/or adult bone marrow—specifically at stages when these tissues support hematopoiesis (Figure 1F). Thus, the niche endothelial signature identified in the CHT is largely conserved both across species and in hematopoietic development.

Endothelial niche-specific *cis*-regulatory elements

To isolate CHT ECs, we generated GFP reporter transgenes using 1.3 or 5.3 kb upstream regulatory sequences for two highly expressed CHT endothelial genes known to promote hematopoietic cell adhesion: *mrc1a* and *sele*.[25,31,32] We then crossed these reporters to the pan-endothelial marker *kdrl:mCherry*. For both the *mrc1a 1.3kb:GFP* and *sele 5.3kb:GFP* transgenes, the highest vascular expression was observed in venous SECs of the CHT, which directly interact with HSPCs and *cxcl12a:dsRed2*+ stromal cells (Figures 2A–2C, S1C, and S1D). Selective GFP expression was similarly observed in kidney marrow ECs (Figures S1E and S1F), consistent with these transgenes marking niche ECs.

To investigate transcriptional control of niche EC-specific gene expression, we dissociated double-positive *mrc1a 1.3kb:GFP*; *kdrl:mCherry* embryos and isolated four populations for RNA-seq and assay for transposase accessible chromatin (ATAC-seq): GFP$^+$; mCherry$^+$ (CHT ECs), GFP$^-$; mCherry$^+$ (non-CHT ECs), GFP$^+$; mCherry$^-$ (mesenchymal cells in the tail fin), and GFP$^-$; mCherry$^-$ (negative remainder of the embryo; Figure 3A). We identified 6,848 regions of chromatin across the genome open in CHT ECs but not the other three cell populations (Table S3). Of the 29 CHT EC genes, 26 had an ATAC-seq element within 100 kb of the transcriptional start site accessible only in CHT ECs (Figure 3B). Similar regions of chromatin accessibility were detected when using the *sele 5.3kb:GFP* transgene (Figure S2A; Table S3). To test whether the uniquely accessible regions of chromatin contain tissue-specific enhancers, we cloned 15 of the elements, fused them to a minimal promoter and GFP, and injected them into zebrafish embryos. 12/15 constructs showed GFP enrichment in CHT ECs at 60–72 hpf (Figure 3B; Table S4). Conversely, 6/6 pan-endothelial ATAC-seq elements (regions that were open and accessible in both EC populations but not the negative or GFP only fractions) drove mosaic GFP expression in ECs throughout the entire embryo (Figure 3C), illustrating the specificity of the CHT elements. Stable integration of several of these enhancer transgenes confirmed the expression observed in F0 animals (Figures 3D and S2B).

To define minimal sequences sufficient to drive CHT EC gene expression, we cloned 125 and 158 bp sequences from the strongest ATAC-seq signal upstream of *mrc1a* and *sele*, respectively (Figures 4A and S2C). When coupled to a minimal promoter, these elements drove GFP expression that was selectively enriched in CHT ECs in 44% (125 bp, *mrc1a*; 155/356) and 23% (158 bp, *sele*; 176/775) of embryos (Figures 4A, S2C, and S2D). On stable integration of each transgene, GFP expression was restricted to CHT ECs (Figures 4B and S2C). Single-cell RNA-seq of FACS-purified ECs from *mrc1a 125bp:GFP*$^+$; *kdrl:mCherry*$^+$ embryos confirmed that GFP$^+$ cells selectively expressed the 29-gene niche endothelial signature (Figure S2E). Transcripts for GFP and some of the 29 genes were also detected in a population of head lymphatic ECs (Figure S2E). However, a direct comparison between the CHT EC and head lymphatic EC populations revealed clear differences in gene expression, including the *bona fide* vascular niche factors *vcam1b*, *cxcl12a*, and *sele*, which were expressed by CHT ECs but not head lymphatic ECs (Figure S2E; Table S5). This expression is consistent with the head lymphatic ECs not recruiting and supporting HSPCs. Within the CHT, *mrc1a 125bp:GFP* expression turned on as HSPCs colonized this tissue, increased in intensity through 8 days post fertilization (dpf), coincident with HSPC expansion, and then decreased steadily as HSPCs exited the CHT (Figure 4C; Video S1). A similar dynamic was observed

(B) Cross-section schematic (upper left) and hierarchical clustering heatmap (upper right) reveal clusters of gene expression that correspond to distinct tissues along the dorsal-ventral axis of the zebrafish tail. Schematic at bottom depicts strategy using *kdrl:GFP* transgenic embryos and FACS to isolate ECs from whole embryos for analysis by RNA-seq.

(C) Graphs show tomo-seq expression traces for individual tissue-specific genes.

(D) Images show whole-mount *in situ* hybridization (WISH) for the pan-endothelial gene *kdrl* (top panel) and CHT EC-enriched genes identified by tomo-seq and tissue-specific RNA-seq (bottom panels). Arrows point to expression in dorsal vasculature and arrowheads point to expression in the CHT.

(E) Heatmap shows the expression of the 29 CHT EC genes in the different cell populations that comprise the adult zebrafish kidney marrow. Spectral scale reports normalized expression.

(F) Heatmap shows the expression of orthologs of the zebrafish CHT EC genes in ECs from different organs of the mouse at different stages of development and postnatal transition to adulthood. Red arrows denote hematopoietic tissues at the respective stage of development. Black bracket denotes genes enriched in fetal liver ECs at the E14–17 stages and then later in the adult bone marrow. Spectral scales report *Z* scores. BM, bone marrow. Scale bars represent 250 μm in this and all subsequent figures unless noted otherwise.

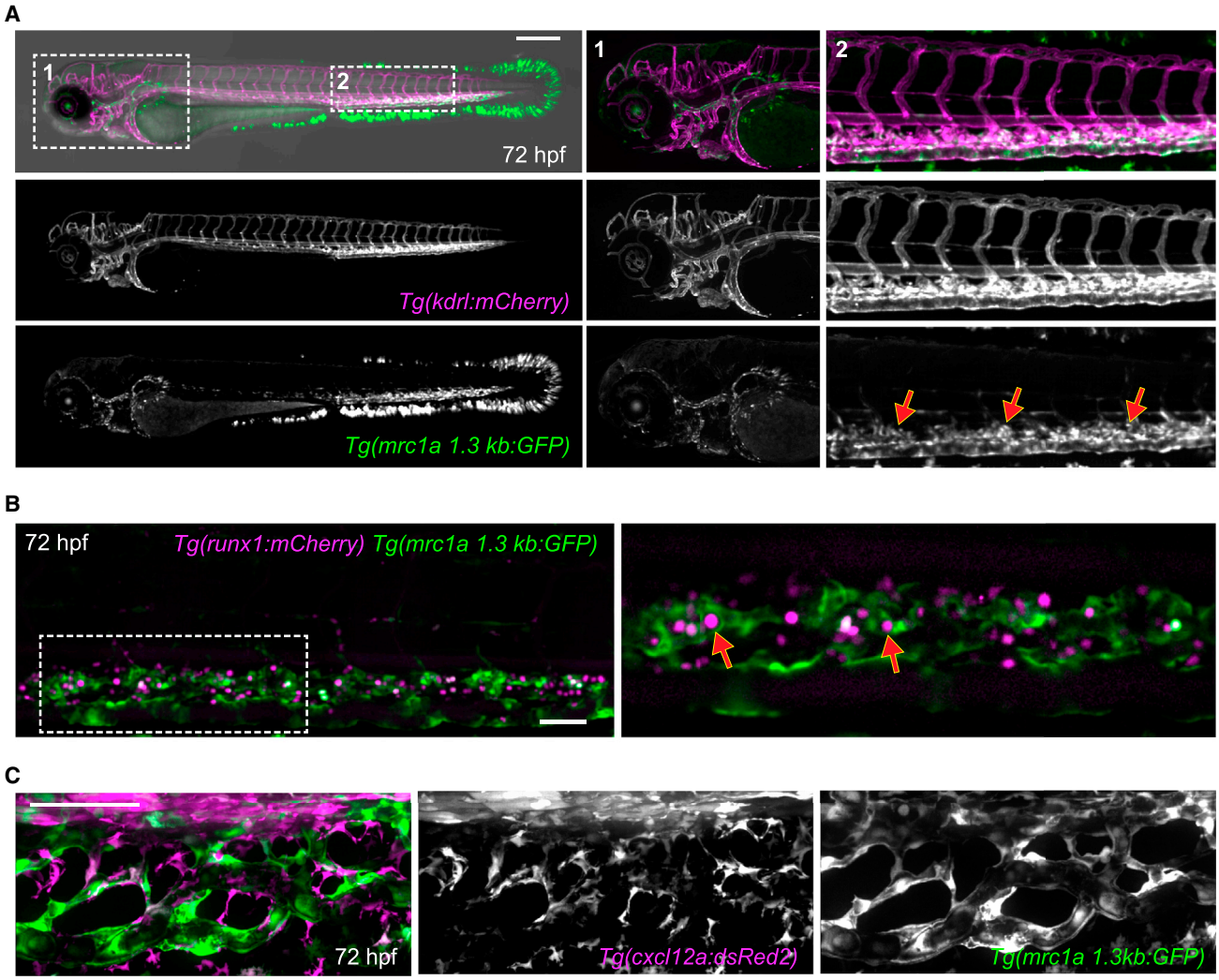

Figure 2. Niche endothelial-enriched *mrc1a 1.3kb:GFP* expression

(A) Images show a double transgenic embryo carrying the pan-endothelial marker *kdrl:mCherry* (magenta) and the *mrc1a 1.3kb:GFP* transgene (green). Magnifications of boxed areas are shown on the right. The highest levels of vascular GFP expression are observed in CHT ECs (red arrows), whereas lower levels of expression are observed in the anterior head region, although some of these cells do not express the *kdrl:mCherry* transgene.

(B) Images show *runx1:mCherry*$^{+}$ HSPCs (magenta) directly interacting with *mrc1a 1.3kb:GFP*$^{+}$ ECs within the CHT niche (red arrows). Panel on right shows magnification of boxed area.

(C) *cxcl12a*:dsRed2^{+} stromal cells (magenta) are closely associated with *mrc1a 1.3kb:GFP*$^{+}$ ECs in the CHT. Scale bars in (B) and (C) represent 100 μm.

in the developing kidney, where GFP expression was observed as HSPCs colonized the kidney (Figure 4C), consistent with a potential role for *mrc1a* in promoting adhesive interactions between HSPCs and the vascular niche.

To identify transcription factors that might bind the CHT EC enhancers, we performed motif enrichment analysis of the 6,848 regions of chromatin uniquely accessible in CHT ECs. This analysis revealed that Ets, SoxF, and nuclear hormone receptor (NR2F2/RORA/RXRA, specifically, abbreviated hereafter as NHR) binding motifs were highly enriched (Figure S2F). In contrast, 4,522 pan-endothelial elements (regions open and accessible in all EC populations) were enriched for Ets, but not SoxF or NHR binding motifs (Figure S2F; Table S3). To test whether the Ets, SoxF, and NHR sites were required for expression, we generated variants of the 125 and 158 bp enhancer sequences with each motif class mutated (Figure 4D; Figure S2G). In each case, a significant reduction or complete loss of GFP expression in CHT ECs was observed (Figures 4E and S2H). GFP expression was unperturbed in embryos injected with control constructs carrying mutations between the Ets, SoxF, and NHR motifs (Figures 4D, 4E, S2G, and S2H). Electrophoretic mobility shift assays demonstrated that NR2F2 (also known as chicken ovalbumin upstream promoter-transcription factor II or [COUP-TFII]), a NHR that promotes venous identity,[33] was able to bind the NHR motifs in the *mrc1a* 125 bp and *sele* 158 bp enhancers (Figure S2I). Together, this work defines a *cis*-regulatory landscape unique to niche ECs and suggests that Ets, Sox, and NHR transcription factors drive niche endothelial development.

CellPress
OPEN ACCESS

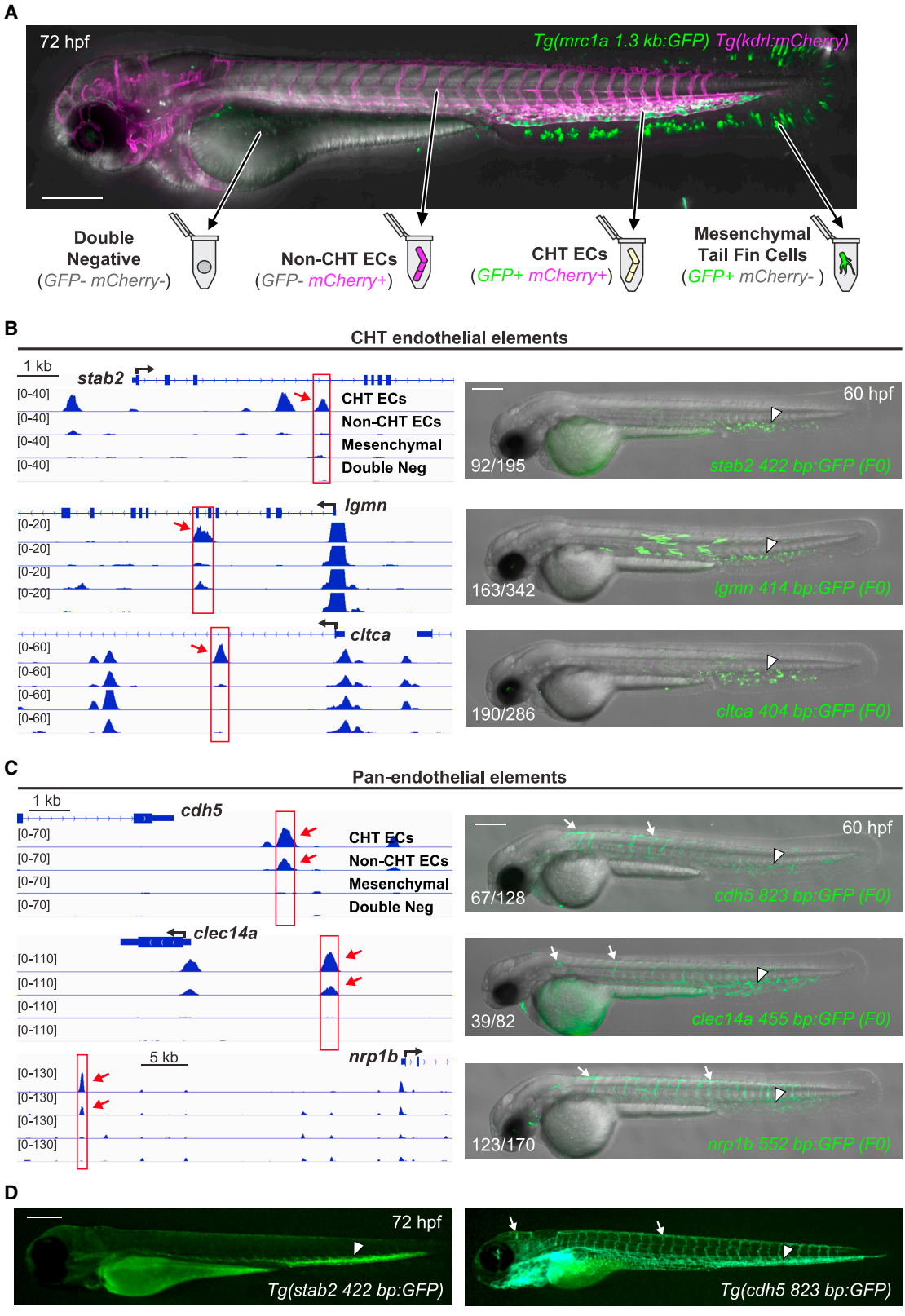

Figure 3. CHT- and pan-endothelial-specific regulatory elements

(A) Image and schematic depict the four cell populations that were isolated from *mrc1a 1.3kb:GFP*$^{+}$; *kdrl:mCherry*$^{+}$ double-positive embryos for analysis by ATAC-seq.

(legend continued on next page)

Defined factors induce niche endothelial expression

To determine the endogenous transcription factors that might bind the Ets, Sox, and NHR motifs *in vivo*, we examined our bulk RNA-seq data from the double-positive CHT ECs. The most highly expressed factors from the Ets, SoxF, and NHR families were *fli1a*, *etv2*, *ets1*, *sox18, sox7*, *nr2f2*, and *rxraa* (Table S6). To test whether a combination of these factors was sufficient to induce ectopic niche endothelial gene expression, we injected a pool of constructs encoding orthologs for the seven factors driven by a ubiquitous (*ubi*) promoter into zebrafish embryos and examined *mrc1a* and *sele* expressions by WISH at 60–72 hpf (Figures 5A–5C). Strikingly, 17% (12/69) of the 7-factor-injected embryos had ectopic *mrc1a* expressions in the head, trunk, and over the yolk, whereas controls did not (0/56; Figures 5B and S3A). Similar results were obtained with WISH for *sele* or when factors were injected into *mrc1a 1.3kb:GFP* and *sele 5.3kb:GFP* embryos (Figures 5C–5E and S3B).

Our mutant-enhancer experiments indicated that at least one factor from each of the three families was required for niche EC gene expression, which led us to ask whether a combination of just three factors, with one from each family, might be sufficient to induce ectopic niche EC gene expression. ETV2 is a pioneer factor essential for the specification of early mesodermal progenitors into vascular cell fates.[34,35] Forced expression of ETV2 in nonvascular cells induces reprogramming toward an early endothelial fate that can generate many types of vasculature.[36–38] Previous work in zebrafish has shown the importance of SoxF factors (*sox7* and *sox18*) and *nr2f2* during arterial-venous specification.[39] We therefore hypothesized that a combination of three of these factors—ETV2, SOX7, and Nr2f2—might be sufficient to induce ectopic niche endothelial gene expression. We injected a pool of *ubi*-driven ETV2, SOX7, and Nr2f2 and observed significant ectopic *mrc1a* expressions, similar to the 7-factor pool (Figures 6A and 6B). Vessels ectopically expressing *mrc1a* had a sinusoidal-like morphology resembling CHT ECs and were functionally integrated into the animal's circulatory system (Figures S3C and S3D; Video S2). These CHT-like ECs similarly showed ectopic expressions of *sele*, *gpr182*, *lgmn*, *stab2*, *ifi30*, *ctsla*, and *hexb*, as well as the *mrc1a 125bp:GFP* transgene, all of which were expressed at levels similar to what is normally observed in the CHT ECs (Figures 6C and 6D). Together, these data provide strong evidence of the cells being reprogrammed into niche ECs. Ectopic *mrc1a* expression was also observed when Sox18 was substituted for SOX7, or ETS1 was substituted for ETV2 (Figures 6A, 6B, S3E, and S3F), suggesting the factors can function interchangeably in terms of reprogramming with the 3-factor pools. Analysis of our single-cell RNA-seq data confirmed the expression of multiple factors from each family within the CHT EC population, with *etv2*, *sox7*, *nr2f1a*, and *nr2f2* showing a higher expression (Figure S4A). To determine whether the individual factors are required for endogenous niche endothelial formation, we sought to use previously published morpholinos (MOs). Knockdown of *etv2* has been shown to cause early vascular abnormalities that preclude its study in later niche formation in the CHT.[35] We found that depletion of both *sox7* and *sox18* together similarly led to early vasculature defects that precluded analysis of the CHT (n = 67/67 animals), although individually they showed no change in *mrc1a 125bp:GFP* expression (n = 90 for *sox7* and 104 for *sox18*). These results were similar to what has been reported previously for *sox7* and *sox18*.[40] MOs targeting each of the *nr2f* family members expressed in CHT ECs (*nr2f1a*, *nr2f2*, and *nr2f5*) showed no effect individually when injected at a low dose, but a combination of all three led to a reduction in *mrc1a 125bp:GFP* expression and fewer HSPCs in the CHT (Figures S4B and S5C). Collectively, these results indicate functional redundancy of the factors for both ectopic niche EC reprogramming activity and endogenous niche formation during development. In the mouse fetal liver (E14–17) and adult bone marrow ECs, multiple factors from the Ets, Sox, and NHR families were expressed, with the highest being *Ets1*, *Sox18*, and *Nr2f2* (Table S7), consistent with the notion that a combination of redundant factors, with at least one from each family (although the specific factors may vary in different species, tissues, and contexts) is a conserved feature of the vascular hematopoietic niche.

To evaluate the contribution of individual transcription factors in our 3-factor overexpression experiments, we injected each factor alone. No single factor alone gave significant ectopic expression, except for ETV2, which led to the ectopic expression of *mrc1a*, although at a lower frequency than with SOX7 and Nr2f2; both of which were required for optimal induction with the ETV2, SOX7, and Nr2f2 3-factor combination (Figures 6B and S3E–S3G). Some of the original seven factors, including *nr2f2* and *ets1*, had endogenous expression in the dorsal tail (Figure S3H), and in most animals injected with ETV2 alone, ectopic expression was restricted to the dorsal tail region, suggesting the ectopic human ETV2 likely works in conjunction with endogenous zebrafish factors in this region. Single-cell RNA-seq analysis of whole zebrafish tails at 72 hpf similarly showed expressions of *etv2*, *sox7*, and *nr2f2* in cells outside the CHT (Figure S4D). Injection of human ETV2 alone induced endogenous zebrafish *sox7, sox18*, *fli1a*, and *etv2* in the dorsal tail region (Figure S3H). By comparison, ectopic expression with the 3-factor combinations was much more widespread and in many tissues, including the anterior head and yolk regions (53% (n = 338/639) of 3-factor injections had ectopic yolk expression compared with 22% (n = 57/265) of ETV2 alone injections), further supporting the notion that the human ETV2, when injected alone, likely works in conjunction with endogenous zebrafish factors to induce ectopic niche EC gene expression. Each of the original seven factors themselves had associated

(B) Gene tracks show regions of chromatin that were uniquely open in the GFP$^+$mCherry$^+$ CHT EC fraction. Images on the right show embryos injected with a CHT EC enhancer-GFP reporter construct corresponding to the red boxed region (red arrow). Arrowheads points to GFP expression in CHT ECs.
(C) Gene tracks show regions of chromatin that were open in both the mCherry$^+$GFP$^+$ (CHT EC) and mCherry$^+$GFP$^-$ (non-CHT EC) populations (red boxes and arrows). Images on the right show embryos injected with pan-endothelial enhancer-GFP reporter constructs corresponding to the red boxed regions. Arrows point to GFP expression in non-CHT ECs and arrowheads point to expression in CHT ECs.
(D) Images show reporter expression of stable enhancer-GFP transgenes. Arrows point to GFP expression in non-CHT ECs and arrowheads point to expression in CHT ECs.

CellPress
OPEN ACCESS

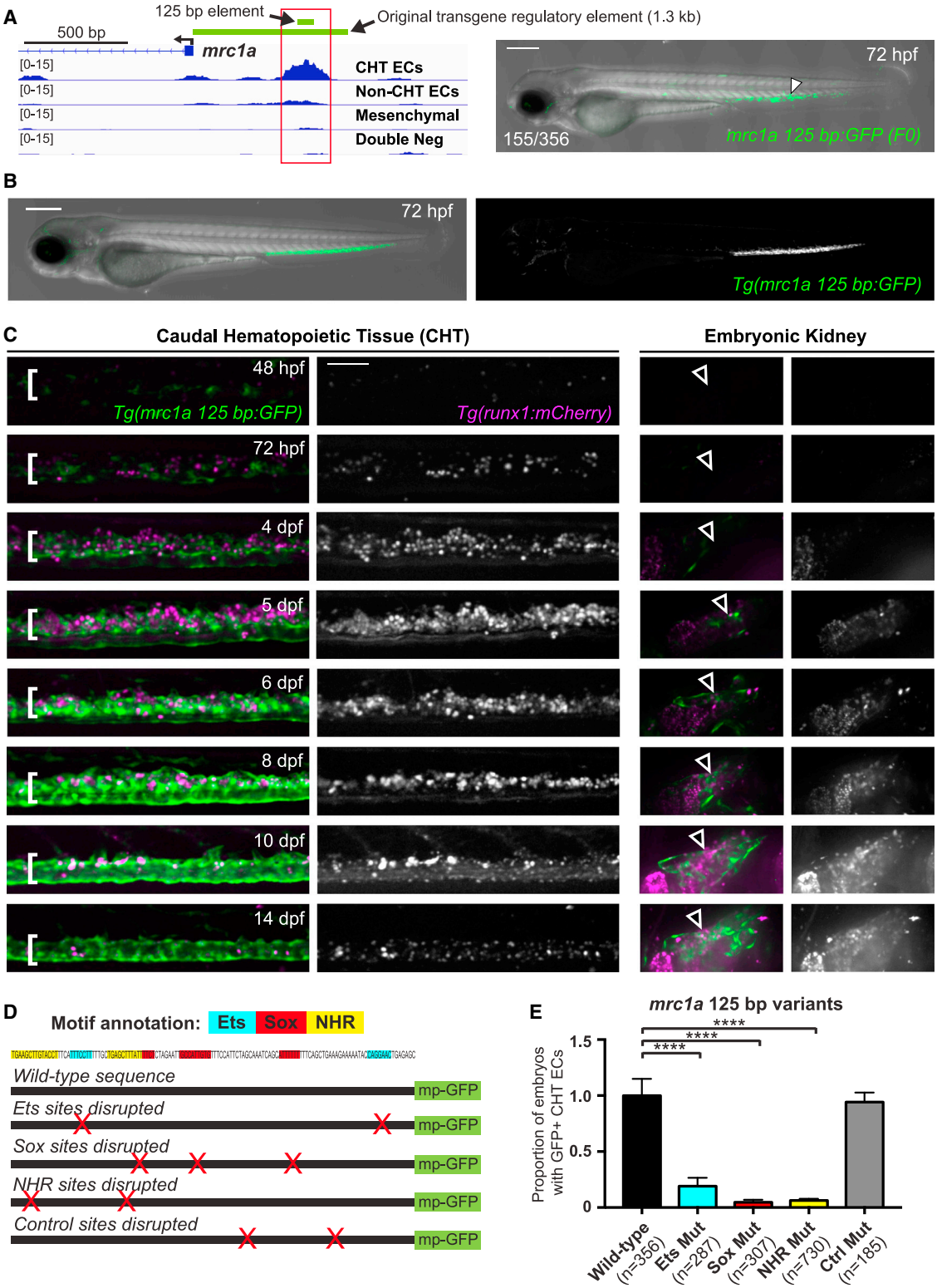

Figure 4. CHT endothelial specific enhancer mutagenesis

(A) Gene tracks show a region of chromatin (red box) upstream of *mrc1a* that is uniquely open in the double-positive CHT EC fraction but not the other three cell populations. Green bars denote the position of the 125 bp enhancer sequence and the 1.3 kb sequence used to generate the reporter transgenes. Image on the right shows transient GFP expression in an F0 embryo injected with the 125 bp enhancer sequence coupled to a minimal promoter and GFP.

(B) Images show an embryo expressing the stably integrated *mrc1a 125 bp:GFP* transgene.

(legend continued on next page)

regions of chromatin uniquely accessible in the CHT EC fraction, harboring Ets, SoxF, and NHR sites (Table S6). Thus, overexpression of the 3-factor combinations likely establishes a reprogramming auto-regulatory loop that drives the niche EC program and underlies the optimal activity of the 3-factor combinations to robustly induce the niche EC program.

As ectopic CHT-like ECs were frequently observed in the dorsal tail, we performed the time-lapse analysis of *ubi*-driven 3-factor injected *mrc1a 125bp:GFP* and *kdrl:mCherry* embryos to determine whether these vessels were outgrowths of CHT vasculature or derived from other cell populations in the embryo. In time-lapse movies, we observed that the ectopic regions were clearly generated independent of the CHT, often prior to the specification of the endogenous CHT ECs (Video S1). Many of the ectopic GFP+ cells appeared to be muscle progenitors based on their size, shape, and location, and these cells often underwent dramatic morphological changes—developing protrusions, becoming migratory and integrating into the vasculature (Videos S3–S6; Figure S5A). Not all cell types exhibited the same behaviors, however. Skin cells and neurons never underwent morphological changes, despite ectopically expressing the *mrc1a 125bp:GFP* transgene (Figure S5B). These observations are consistent with studies showing that muscle progenitors in the zebrafish embryo are susceptible to reprogramming to an endothelial fate by *etv2* overexpression.[38] As the *ubi* promoter is active very early in development, we sought to evaluate whether niche ECs could be induced at a later stage of development. We injected constructs with ETV2, SOX7, and Nr2f2 downstream of a heat shock promoter (*hsp70l*). Heat shock induction at 24 hpf resulted in large patches of niche EC gene expression throughout the animal; by 48 h post-heat shock, these cells incorporated into the vasculature (Figure S5C). To test whether the CHT EC program could be induced specifically in muscle cells, we used the muscle-specific *mylz2* promoter to drive the expression of the 3-factor pool. We observed *mrc1a 125bp:GFP*$^+$ muscle cells co-expressing the vascular marker *kdrl:mCherry*, often undergoing morphological changes (n = 33/60 animals; Figure 6E). To test whether the CHT EC program could be induced specifically in non-CHT ECs at later stages of development, we overexpressed the 3-factor pool using the pan-endothelial *nrp1b* enhancer that we had isolated earlier. In these animals, we observed ectopic *mrc1a 125bp:GFP* expression in non-CHT ECs, including AECs (n = 22/87 animals; Figures 6E and S5D). The amount of ectopic expression per embryo with the *mylz2* and *nrp1b* drivers was noticeably less than with the *ubi*-driven factors, likely reflective of these drivers turning on later, in more differentiated cell types (differentiated muscle and vasculature, respectively; Figure 6E). Collectively, these data indicate that the minimal combination of Ets, SoxF, and NHR factors is sufficient to induce CHT EC gene expression in multiple cell types at different stages of development, with muscle progenitors being particularly susceptible to trans-differentiation into CHT-like ECs.

Ectopic vascular regions recruit HSPCs and support their proliferation

We next asked whether the ectopic CHT-like ECs were capable of recruiting and supporting HSPCs outside of the endogenous CHT. Injection of 3-factor pools (ETV2 or ETS1 with SOX7 and Nr2f2) under the control of the *ubi* promoter resulted in *runx1*$^+$ HSPCs localized outside of the CHT (Figures 7A, 7B, and S5E). 12/22 embryos with ectopic vascular patches of *mrc1a 1.3kb:GFP* contained *runx1:mCherry*$^+$ cells often with multiple HSPCs localized within the ectopic regions. In contrast, only 5/48 control embryos had HSPC localization outside the CHT. The *ubi*-induced ectopic *mrc1a:GFP*$^+$ ECs often formed pockets around the HSPCs and were associated with *cxcl12a:dsRed2*$^+$ stromal cells and *mpeg1:mCherry*+ macrophages, similar to CHT ECs (Figures 7B, 7C, and S5F; Videos S7–S9). We did not observe stromal cells or HSPCs localized to ectopic CHT-like vessels in the head or over the yolk (Figure S5G), suggesting specificity in the anatomical location and/or a functional requirement of other cells in the tail (e.g., stromal cells) for the ectopic niche activity.

To investigate the dynamics of the ectopic HSPCs localized outside of the CHT, we used time-lapse microscopy. In control embryos, the majority of HSPCs observed outside the CHT were only transiently localized and only one division outside of the CHT was observed in 10 embryos (Figure S5H). In contrast, HSPCs localized to ectopic CHT-like ECs for several hours in 3-factor-injected embryos and divided at rates similar to HSPCs in the endogenous CHT niche (6 divisions observed in 10 embryos; 5/6 divisions corresponded to HSPCs with residency times over 2.5 h; Figure S5H).[20] We visualized recruitment, lodging, and division of HSPCs but did not observe HSPC formation at the ectopic sites (Figure 7D; Video S8). When HSPCs divided, daughter cells migrated away and entered circulation, similar to what is observed in the CHT, presumably traveling to subsequent niches (Video S9). Thus, multiple HSPC behaviors normally restricted to the endogenous CHT were exhibited in the ectopic patches of CHT-like ECs. Together, these data demonstrate that a minimal combination of Ets, Sox, and NHR factors can induce ectopic niche ECs that associate with *cxcl12a*+ stromal cells and support the recruitment, maintenance, and division of HSPCs outside the endogenous niche.

DISCUSSION

Our data support a model in which Ets, Sox, and NHR factors are sufficient to specify the identity and capacity of vascular niche

(C) Images show *mrc1a 125bp:GFP* (green) and *runx1:mCherry* (magenta) expression in the CHT (left) and kidney (right) at 8 different developmental time points. White brackets denote the location of the CHT and arrowheads point to the location of the developing kidney. Grayscale images of the *runx1:mCherry* signal are shown to the right of color overlays. Identical settings were used for image acquisition at each time point. The fluorescence intensity for the images in the figure was adjusted relative to the highest expression at 8 dpf. This results in the reduced fluorescence intensity in the image for the 48 hpf time point.

(D) Wild-type sequence of the 125 bp *mrc1a* enhancer is shown, annotated with colors highlighting the Ets, Sox, and NHR binding motifs. Schematic depicts enhancer-reporter constructs in which each class of motif or control regions was targeted by mutation. Red X's denote the location of targeted sites. mp-GFP, mouse *Beta-globin* minimal promoter fused to GFP.

(E) Graphs report the frequency of embryos with GFP expression in CHT ECs after injection with wild-type sequences or mutated variants of the *mrc1a* 125 bp enhancer. Data is normalized to the wild-type control (44% [155/356]). Mean ± SEM, one-way ANOVA with Dunnett's multiple comparisons test; ***$p < 0.001$, ****$p < 0.0001$. All experiments were performed at least three times, with independent clutches. Scale bar in (C) represents 100 μm.

CellPress
OPEN ACCESS

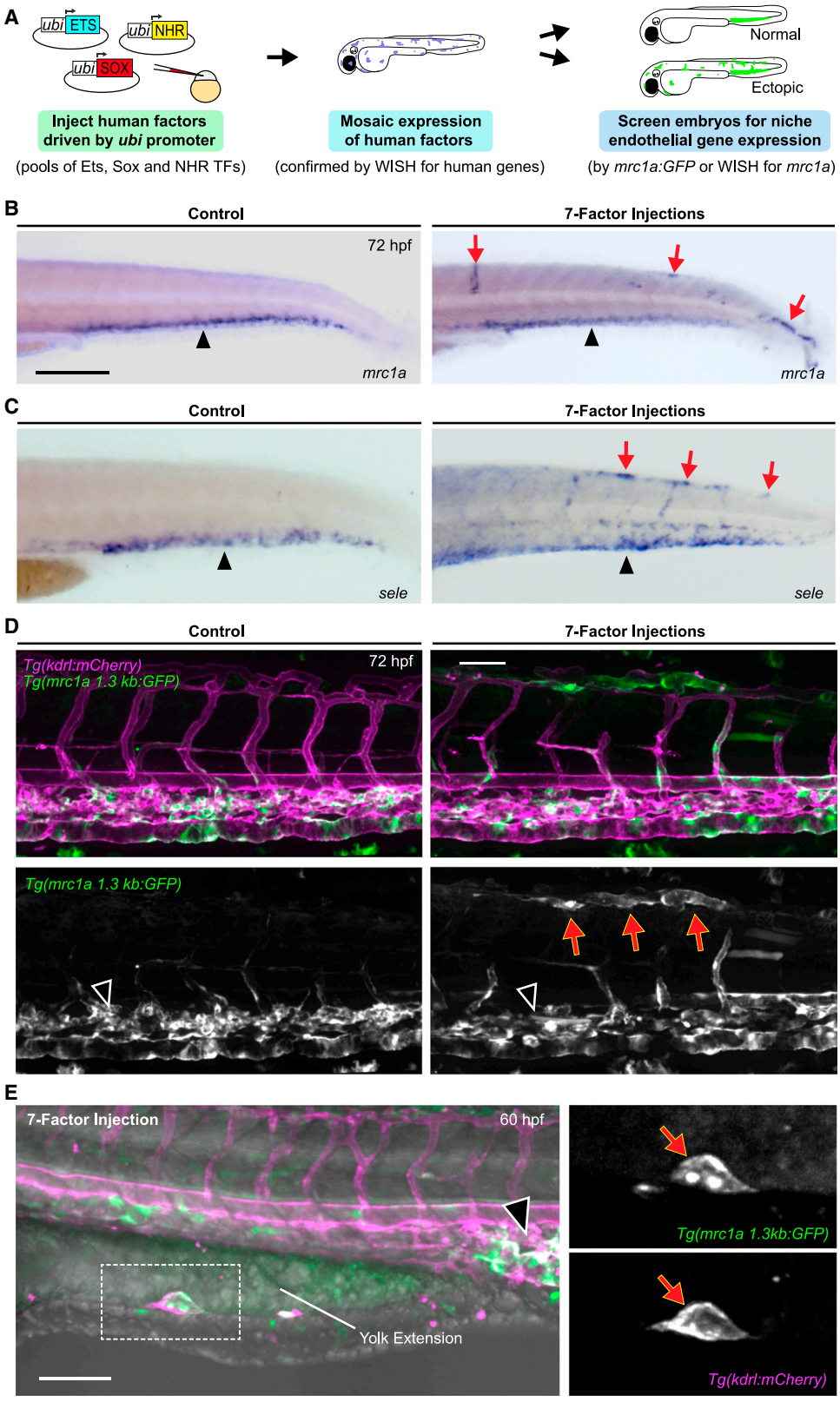

(legend on next page)

ECs, which likely work in conjunction with other niche cell types to recruit and support the proliferation of blood stem cells. Based on conserved gene expression, similar mechanisms appear to be in place in hematopoietic niche ECs across species and development. Other transcription factors including Tfec and Klf6a[24,26] have been shown to drive CHT vascular gene expression that maintains hematopoietic cells. These factors were not identified by our study here but are known to turn on much earlier in development such that we might have missed them with our analysis at 72 hpf. Of note, several of the transcription factors we did identify are expressed more broadly in venous vasculature earlier in development but not all veins express the niche signature, consistent with a model where multiple factors in the CHT ECs are required for niche EC gene expression. The niche endothelial signature identified here includes genes that regulate adhesive interactions between ECs and circulating cells (e.g., the adhesion receptor E-selectin[25,32] and the scavenger receptors *mrc1a*, *stab1*, and *stab2*[31,41,42]). Another CHT niche EC gene, *gpr182*, was recently shown to be a vascular niche-expressed receptor that maintains HSPC homeostasis in fish and mice.[43,44] Our studies identified other *bona fide* niche factors including *vcam1b* and *cxcl12a* as being expressed by the niche ECs. In the bone marrow niche, these genes are expressed by multiple cell types, including ECs, macrophages, and mesenchymal stromal cells. This appears to be the same in the CHT niche as *cxcl12a* also marks mesenchymal stromal cells[45] and *vcam1b* was recently reported to function in macrophages within the CHT niche.[16] Of note, there was not an obvious set of genes within our signature that would promote HSPC expansion. It is possible that our transcription factor cocktail might not regulate every aspect of CHT vascular identity, and such factors are expressed by the other cells we see associated with the ectopic niches. There are numerous genes identified by this study that were not previously associated with the HSPC niche, including several with activities related to endocytosis and membrane trafficking: *ap1b1*, *dab2*, *pxk*, *exoc3l2a*, and *snx8*. Validating our expression analysis, ECs in the CHT were recently shown to be highly endocytic.[46] This endocytic activity might regulate ligand/receptor turnover or may clear potentially harmful agents, such as waste products, modified proteins, or microbial material from the niche.

Recent analyses of the mammalian HSPC niche comparing gene expression between SECs and AECs[10,47,48] show an overlap between our niche EC signature and venous SECs in the mouse bone marrow. Although AECs may also support hematopoiesis,[8,9,49] our work illustrates the capacity of SECs to recruit HSPCs and support their division. Stress-induced extramedullary hematopoiesis may involve the induction of this SEC niche program. A number of our niche EC genes were enriched in adult mouse liver ECs (Figure 1E), suggesting the liver may be partially 'primed' to support hematopoiesis under stress. Our work here highlights shared gene expression between niche ECs and head lymphatic vessels in the zebrafish embryo. Although these head lymphatic vessels in the fish do not support HSPCs, it was recently shown that lymphatic vessels are a supportive component of the hair follicle stem cell niche.[50]

Our overexpression studies indicate that 3-factor combinations of Ets, SoxF, and NHR transcription factors—where specific family members are interchangeable—are able to induce niche EC gene expression in different cell types, including AECs, muscle, and ectodermal lineages (skin cells and neurons). Some cell populations appear to be more refractory to reprogramming, whereas others (e.g., muscle progenitors) trans-differentiate into CHT-like ECs with functional niche properties. The susceptibility of muscle progenitors to reprogramming might be tied to the chromatin state and/or differentiation status of the cells or may be related to the shared mesodermal origin of muscle and ECs. Such reprogrammed niche ECs might be used in conjunction with reprogrammed stromal cells[51] to enhance the production, maintenance, or expansion of HSPCs *in vitro*. Parabiosis experiments indicate that niche size determines HSPC number,[52] and functional ectopic niches, termed ossicles, have been used to assemble a bone marrow equivalent upon transplantation[53,54]; it is likely that these structures contain SECs. These studies, in combination with our work here, establish the concept that HSPC numbers could be supported *in vivo* using a reprogramming-based niche therapy to generate ectopic vascular niches at new safe harbor locations in the body, particularly for blood diseases like myelofibrosis in which the normal bone marrow niche no longer functions properly. Such a synthetic niche in the long-term may function normally or be associated with some dysregulation requiring further development of the system. Nevertheless, this would be a potential therapy for relocating and stimulating hematopoietic stem cells. Collectively, our work here advances the fundamental understanding of the vascular niche that choreographs homeostasis and regeneration of blood stem cells, which may guide strategies to culture and expand HSPCs for transplantation.

Limitations of the study

Of note, our study here has certain limitations. Although muscle progenitors are likely to be a major contributor, we cannot conclude definitively with our current data the source of embryonic cells giving rise to the ectopic CHT-like ECs. Similarly, we have not yet rigorously assessed the full capacity of the ectopic niches to support HSPCs, compared with the endogenous niche

Figure 5. 7-factor induction of ectopic niche EC gene expression

(A) Schematic depicts the strategy used in transcription factor overexpression experiments.

(B and C) Images show embryos that were injected with control DNA (left) or a pool of seven transcription factors (right) from the Ets, Sox, and NHR families (FLI1, ETV2, ETS1, SOX7, Sox18, Nr2f2, and RXRA) and then stained by WISH for *mrc1a* (B) or *sele* (C). Red arrows denote regions of ectopic expression and black arrowheads point to normal domains of expression in all panels of this figure.

(D) Images show *mrc1a 1.3kb:GFP*; *kdrl:mCherry* double transgenic embryos that were injected with control DNA (left) or a pool of seven transcription factors (right).

(E) Images show ectopic expression of the *mrc1a 1.3kb:GFP* and *kdrl:mCherry* transgenes over the yolk extension in a 7-factor injected embryo. Magnification of the boxed area is shown at the right. Control and experimental groups were blinded prior to scoring and all experiments were performed at least three times, with independent clutches. Scale bars in (D) and (E) represent 100 μm.

CellPress
OPEN ACCESS

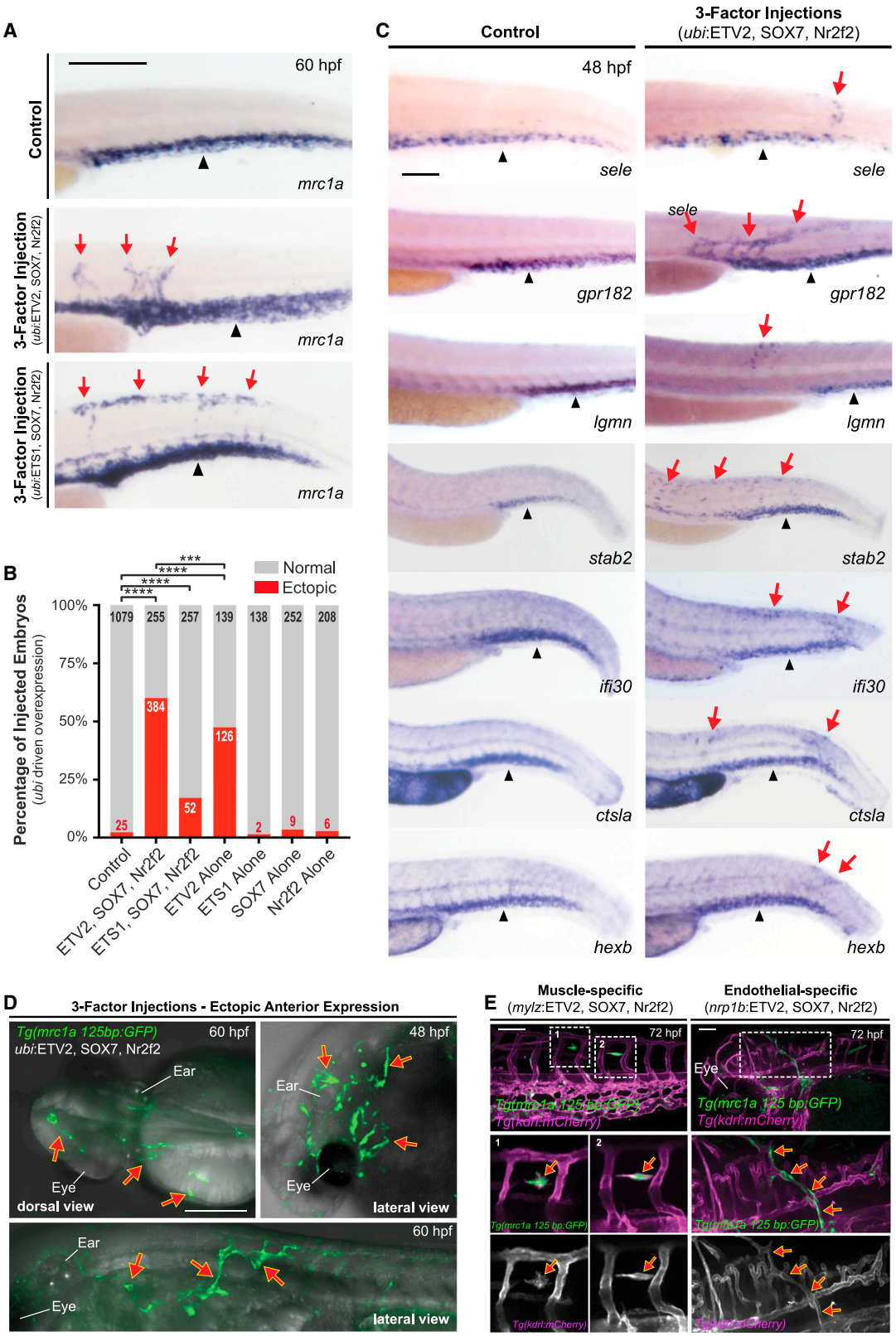

Figure 6. 3-factor induction of ectopic niche EC gene expression

(A) Images show WISH for *mrc1a* in a control embryo (top) or after injection of a 3-factor pool containing ETV2, SOX7 and Nr2f2 (middle) or ETS1, SOX7, and Nr2f2 (bottom). Black arrowheads point to endogenous expression while red arrows point to ectopic expression in all panels of this figure.

(legend continued on next page)

in the CHT. Both questions will require the development and/or implementation of tools that are beyond the scope of the present study. Finally, it remains to be determined whether the cocktail of transcription factors defined here will exhibit the same degree of transdifferentiating activity in human cells. Nonetheless, our study advances the fundamental understanding of the mechanisms that underlie niche function, providing a conceptual framework for future "niche therapies" for the treatment of numerous hematopoietic disorders including cancer.

STAR★METHODS

Detailed methods are provided in the online version of this paper and include the following:

- KEY RESOURCES TABLE
- RESOURCE AVAILABILITY
  - Lead contact
  - Materials availability
  - Data and code availability
- EXPERIMENTAL MODEL AND SUBJECT DETAILS
  - Animals
- METHOD DETAILS
  - Genomic analyses
  - Whole mount *in situ* hybridization (WISH)
  - Transgenesis and enhancer-GFP reporter assays
  - Transcription factor overexpression studies
  - Microscopy and image analysis
  - Flow cytometry, kidney marrow dissection, dissociation, and histology
  - Morpholino injections
  - Electrophoretic mobility shift assay
- QUANTIFICATION AND STATISTICAL ANALYSIS

SUPPLEMENTAL INFORMATION

Supplemental information can be found online at https://doi.org/10.1016/j.devcel.2023.04.007.

ACKNOWLEDGMENTS

This work was supported by HHMI and NIH grants R01 HL04880, U54 DK110805, U01 HL100001, R24 DK092760, U01 HI134812, P01 HL131477, and RC2DK120535, and a Harvard Catalyst grant to L.I.Z. E.J.H. was an HHMI Fellow of the Helen Hay Whitney Foundation and is supported by NIH grant K01 DK111790. J.R.P. was supported by an ACS fellowship (127868-PF-15-128-01-DDC). B.K. is supported by NIH T32 HD060600. T.T.D. is supported by NIH grant T32 HL098049 and an AHA Postdoctoral Fellowship. E.C.B. is supported by NIH grant R01 AI130471 and award I01 BX-002919 from the Department of Veterans Affairs. We gratefully acknowledge the aquatics research staff at BCH, in particular, K. Maloney, S. Hurley, and C. Lawrence. We thank R. Mathieu and M. Paktinat in the BCH flow cytometry core and M. Chatterjee in the Single Cell Core at Harvard for help with inDrops single-cell RNA-seq. We thank J. Henninger for assistance with kidney marrow dissections and E. Fast and A. McConnell for comments on the manuscript.

AUTHOR CONTRIBUTIONS

E.J.H. designed the study, funded the project, performed experiments, managed the project, interpreted the data, and wrote the manuscript. J.R.P. designed the study, performed experiments, managed the project, interpreted the data, and edited the manuscript. R.J.F. S.J.W., C.M., I.F.-M., M.L.D, C.D., T.H., M.J.F, J.W.K., R.R., B.L., D.A.V.E.R., K.E, E.L.H., H.G.W., S.E.R., S.H.C., B.K., J.M.G.-S., T.T.D., J.P., and J.P.J performed experiments and provided technical support. A.L., S.Y., and Y.Z. provided bioinformatics support. H.A.F provided biostatistics support. E.C.B, A.v.O., J.P.J., and S.R. funded and supervised the project. L.I.Z. designed the study, funded and supervised the project, interpreted the data, and edited the manuscript. All authors reviewed the manuscript.

DECLARATION OF INTERESTS

L.I.Z. is a founder and stockholder of Fate Therapeutics, CAMP4 Therapeutics, and Scholar Rock. He is a consultant for Celularity.

INCLUSION AND DIVERSITY

We support inclusive, diverse, and equitable conduct of research.

Received: October 19, 2022
Revised: February 8, 2023
Accepted: April 7, 2023
Published: April 28, 2023

REFERENCES

1. Orkin, S.H., and Zon, L.I. (2008). Hematopoiesis: an evolving paradigm for stem cell biology. Cell *132*, 631–644.
2. Ding, L., Saunders, T.L., Enikolopov, G., and Morrison, S.J. (2012). Endothelial and perivascular cells maintain haematopoietic stem cells. Nature *481*, 457–462.
3. Heissig, B., Hattori, K., Dias, S., Friedrich, M., Ferris, B., Hackett, N.R., Crystal, R.G., Besmer, P., Lyden, D., Moore, M.A., et al. (2002). Recruitment of stem and progenitor cells from the bone marrow niche requires MMP-9 mediated release of kit-ligand. Cell *109*, 625–637.
4. Kiel, M.J., Yilmaz, O.H., Iwashita, T., Yilmaz, O.H., Terhorst, C., and Morrison, S.J. (2005). SLAM family receptors distinguish hematopoietic stem and progenitor cells and reveal endothelial niches for stem cells. Cell *121*, 1109–1121.
5. Perlin, J.R., Sporrij, A., and Zon, L.I. (2017). Blood on the tracks: hematopoietic stem cell-endothelial cell interactions in homing and engraftment. J. Mol. Med. (Berl) *95*, 809–819.
6. Sugiyama, T., Kohara, H., Noda, M., and Nagasawa, T. (2006). Maintenance of the hematopoietic stem cell pool by CXCL12-CXCR4 chemokine signaling in bone marrow stromal cell niches. Immunity *25*, 977–988.
7. Wei, Q., and Frenette, P.S. (2018). Niches for hematopoietic stem cells and their progeny. Immunity *48*, 632–648.

(B) Graph reports quantification of the percentage of injected embryos that displayed ectopic *mrc1a* WISH staining after transcription factor overexpression. Chi-squared test and Fisher's exact test for pairwise comparisons with the Holm step-down process to correct for multiple comparisons; ***$p < 0.001$, ****$p < 0.0001$.
(C) Images show WISH for CHT niche EC genes in control embryos (left) and embryos injected with the 3-factor *ubi*:ETV2, SOX7, and Nr2f2 combination (right).
(D) Images show ectopic GFP expression in vessels in the anterior head and yolk region of *mrc1a 125bp:GFP* transgenic embryos injected with the 3-factor *ubi*:ETV2, SOX7, and Nr2f2 mixtures.
(E) Images show ectopic expression in *mrc1a 125bp:GFP; kdrl:mCherry* double-positive embryos that were injected with muscle-specific *mylz2:*ETV2, SOX7, Nr2f2 (left), or endothelial-specific *nrp1b:*ETV2, SOX7, and Nr2f2 (right) plasmids. Magnification of boxed regions is shown at the bottom. Control and experimental groups were blinded prior to scoring and all experiments were performed at least three times, with independent clutches. Scale bars in (C) and (E) represent 100 μm.

CellPress
OPEN ACCESS

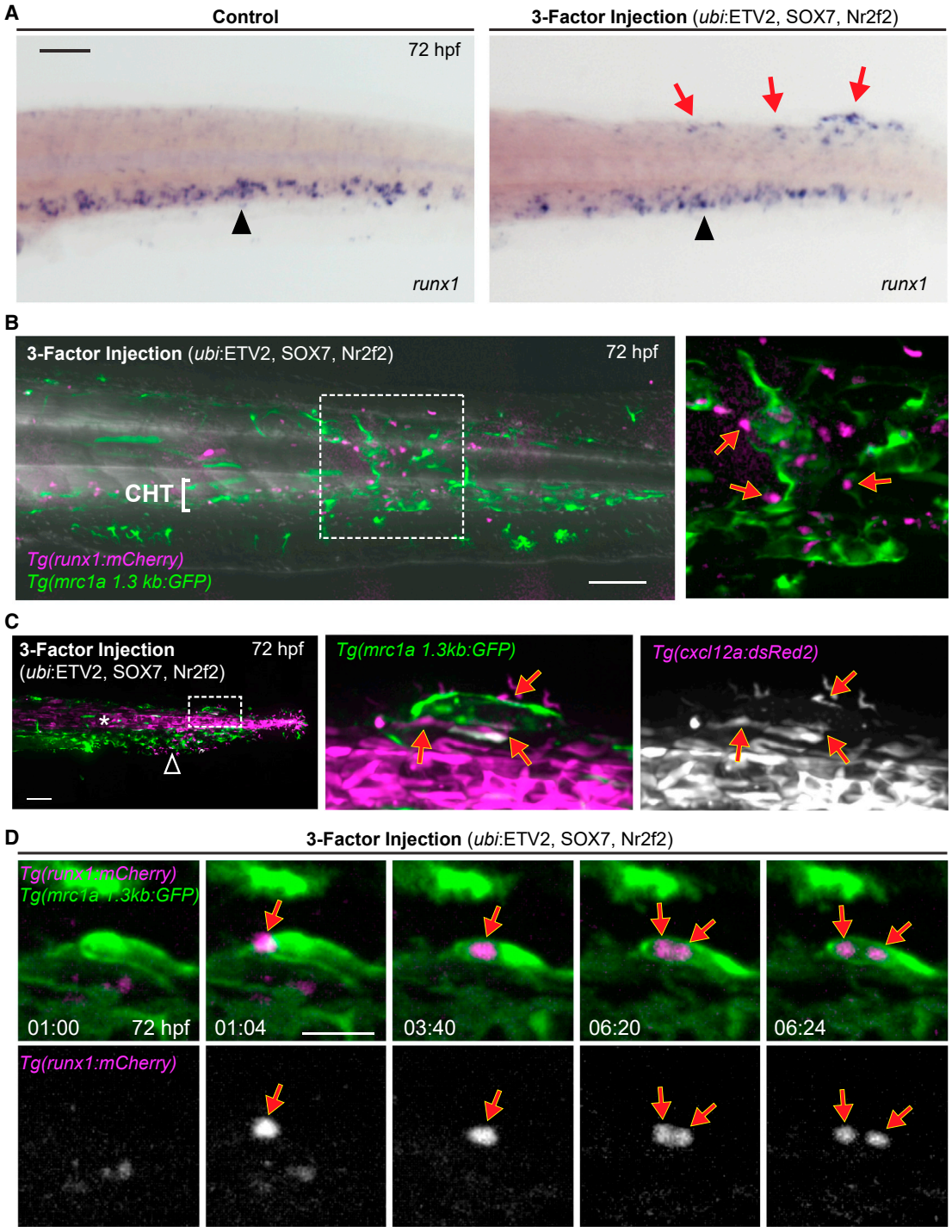

Figure 7. Ectopic vascular regions recruit HSPCs and support their proliferation

(A) WISH for *runx1* shows HSPC localization in a control (left) and 3-factor injected embryo (right). Black arrowheads denote endogenous CHT localization; and red arrows point to ectopic localization.

(B) Image shows *runx1:mCherry*$^{+}$ HSPCs localized outside the CHT within a large ectopic region of *mrc1a 1.3kb:GFP* expression in an embryo injected with a pool of *ubi*:ETV2, SOX7, and Nr2f2. Magnification of boxed area is shown on the right.

(C) ECs ectopically expressing *mrc1a 1.3kb:GFP* are associated with *cxcl12a:dsRed2*$^{+}$ stromal cells, similar to ECs in the CHT. Asterisk denotes notochord expression of *cxcl12a*:dsRed2, and the black arrowhead points to CHT localization. Magnification of boxed region is shown.

(D) Time-lapse series shows a *runx1:mCherry*$^{+}$ HSPC (red arrows) initially arriving at an ectopic site and subsequently dividing (images show magnification of region with red arrow in Video S8). Time is shown as hh:mm. Control and experimental groups were blinded prior to scoring and all experiments were performed at least three times, with independent clutches. Scale bars represent 100 μm in (A-C), and 30 μm in (D).

8. Itkin, T., Gur-Cohen, S., Spencer, J.A., Schajnovitz, A., Ramasamy, S.K., Kusumbe, A.P., Ledergor, G., Jung, Y., Milo, I., Poulos, M.G., et al. (2016). Distinct bone marrow blood vessels differentially regulate haematopoiesis. Nature *532*, 323–328.

9. Kunisaki, Y., Bruns, I., Scheiermann, C., Ahmed, J., Pinho, S., Zhang, D., Mizoguchi, T., Wei, Q., Lucas, D., Ito, K., et al. (2013). Arteriolar niches maintain haematopoietic stem cell quiescence. Nature *502*, 637–643.

10. Xu, C., Gao, X., Wei, Q., Nakahara, F., Zimmerman, S.E., Mar, J., and Frenette, P.S. (2018). Stem cell factor is selectively secreted by arterial endothelial cells in bone marrow. Nat. Commun. *9*, 2449.

11. Avecilla, S.T., Hattori, K., Heissig, B., Tejada, R., Liao, F., Shido, K., Jin, D.K., Dias, S., Zhang, F., Hartman, T.E., et al. (2004). Chemokine-mediated interaction of hematopoietic progenitors with the bone marrow vascular niche is required for thrombopoiesis. Nat. Med. *10*, 64–71.

12. Hooper, A.T., Butler, J.M., Nolan, D.J., Kranz, A., Iida, K., Kobayashi, M., Kopp, H.G., Shido, K., Petit, I., Yanger, K., et al. (2009). Engraftment and reconstitution of hematopoiesis is dependent on VEGFR2-mediated regeneration of sinusoidal endothelial cells. Cell Stem Cell *4*, 263–274.

13. Kim, C.H. (2010). Homeostatic and pathogenic extramedullary hematopoiesis. J. Blood Med. *1*, 13–19.

14. Murayama, E., Kissa, K., Zapata, A., Mordelet, E., Briolat, V., Lin, H.F., Handin, R.I., and Herbomel, P. (2006). Tracing hematopoietic precursor migration to successive hematopoietic organs during zebrafish development. Immunity *25*, 963–975.

15. Wiley, D.M., Kim, J.D., Hao, J., Hong, C.C., Bautch, V.L., and Jin, S.W. (2011). Distinct signalling pathways regulate sprouting angiogenesis from the dorsal aorta and the axial vein. Nat. Cell Biol. *13*, 686–692.

16. Li, D., Xue, W., Li, M., Dong, M., Wang, J., Wang, X., Li, X., Chen, K., Zhang, W., Wu, S., et al. (2018). VCAM-1(+) macrophages guide the homing of HSPCs to a vascular niche. Nature *564*, 119–124. https://doi.org/10.1038/s41586-018-0709-7.

17. Tamplin, O.J., Durand, E.M., Carr, L.A., Childs, S.J., Hagedorn, E.J., Li, P., Yzaguirre, A.D., Speck, N.A., and Zon, L.I. (2015). Hematopoietic stem cell arrival triggers dynamic remodeling of the perivascular niche. Cell *160*, 241–252.

18. Xue, Y., Liu, D., Cui, G., Ding, Y., Ai, D., Gao, S., Zhang, Y., Suo, S., Wang, X., Lv, P., et al. (2019). A 3D atlas of hematopoietic stem and progenitor cell expansion by multi-dimensional RNA-seq analysis. Cell Rep. *27*, 1567–1578.e5.

19. Murayama, E., Sarris, M., Redd, M., Le Guyader, D., Vivier, C., Horsley, W., Trede, N., and Herbomel, P. (2015). NACA deficiency reveals the crucial role of somite-derived stromal cells in haematopoietic niche formation. Nat. Commun. *6*, 8375.

20. Blaser, B.W., Moore, J.L., Hagedorn, E.J., Li, B., Riquelme, R., Lichtig, A., Yang, S., Zhou, Y., Tamplin, O.J., Binder, V., and Zon, L.I. (2017). CXCR1 remodels the vascular niche to promote hematopoietic stem and progenitor cell engraftment. J. Exp. Med. *214*, 1011–1027.

21. Butler, J.M., Nolan, D.J., Vertes, E.L., Varnum-Finney, B., Kobayashi, H., Hooper, A.T., Seandel, M., Shido, K., White, I.A., Kobayashi, M., et al. (2010). Endothelial cells are essential for the self-renewal and repopulation of Notch-dependent hematopoietic stem cells. Cell Stem Cell *6*, 251–264.

22. Ding, L., and Morrison, S.J. (2013). Haematopoietic stem cells and early lymphoid progenitors occupy distinct bone marrow niches. Nature *495*, 231–235.

23. Greenbaum, A., Hsu, Y.M., Day, R.B., Schuettpelz, L.G., Christopher, M.J., Borgerding, J.N., Nagasawa, T., and Link, D.C. (2013). CXCL12 in early mesenchymal progenitors is required for haematopoietic stem-cell maintenance. Nature *495*, 227–230.

24. Mahony, C.B., Fish, R.J., Pasche, C., and Bertrand, J.Y. (2016). tfec controls the hematopoietic stem cell vascular niche during zebrafish embryogenesis. Blood *128*, 1336–1345.

25. Winkler, I.G., Barbier, V., Nowlan, B., Jacobsen, R.N., Forristal, C.E., Patton, J.T., Magnani, J.L., and Lévesque, J.P. (2012). Vascular niche E-selectin regulates hematopoietic stem cell dormancy, self renewal and chemoresistance. Nat. Med. *18*, 1651–1657.

26. Xue, Y., Lv, J., Zhang, C., Wang, L., Ma, D., and Liu, F. (2017). The vascular niche regulates hematopoietic stem and progenitor cell lodgment and expansion via klf6a-ccl25b. Dev. Cell *42*, 349–362.e4.

27. Junker, J.P., Noël, E.S., Guryev, V., Peterson, K.A., Shah, G., Huisken, J., McMahon, A.P., Berezikov, E., Bakkers, J., and van Oudenaarden, A. (2014). Genome-wide RNA Tomography in the zebrafish embryo. Cell *159*, 662–675.

28. Theodore, L.N., Hagedorn, E.J., Cortes, M., Natsuhara, K., Liu, S.Y., Perlin, J.R., Yang, S., Daily, M.L., Zon, L.I., and North, T.E. (2017). Distinct roles for matrix metalloproteinases 2 and 9 in embryonic hematopoietic stem cell emergence, migration, and niche colonization. Stem Cell Rep. *8*, 1226–1241.

29. Zapata, A. (1979). Ultrastructural study of the teleost fish kidney. Dev. Comp. Immunol. *3*, 55–65.

30. Barry, D.M., McMillan, E.A., Kunar, B., Lis, R., Zhang, T., Lu, T., Daniel, E., Yokoyama, M., Gomez-Salinero, J.M., Sureshbabu, A., et al. (2019). Molecular determinants of nephron vascular specialization in the kidney. Nat. Commun. *10*, 5705.

31. Irjala, H., Johansson, E.L., Grenman, R., Alanen, K., Salmi, M., and Jalkanen, S. (2001). Mannose receptor is a novel ligand for L-selectin and mediates lymphocyte binding to lymphatic endothelium. J. Exp. Med. *194*, 1033–1042.

32. Frenette, P.S., Mayadas, T.N., Rayburn, H., Hynes, R.O., and Wagner, D.D. (1996). Susceptibility to infection and altered hematopoiesis in mice deficient in both P- and E-selectins. Cell *84*, 563–574.

33. Aranguren, X.L., Beerens, M., Vandevelde, W., Dewerchin, M., Carmeliet, P., and Luttun, A. (2011). Transcription factor COUP-TFII is indispensable for venous and lymphatic development in zebrafish and Xenopus laevis. Biochem. Biophys. Res. Commun. *410*, 121–126.

34. De Val, S., Chi, N.C., Meadows, S.M., Minovitsky, S., Anderson, J.P., Harris, I.S., Ehlers, M.L., Agarwal, P., Visel, A., Xu, S.M., et al. (2008). Combinatorial regulation of endothelial gene expression by ets and forkhead transcription factors. Cell *135*, 1053–1064.

35. Sumanas, S., and Lin, S. (2006). Ets1-related protein is a key regulator of vasculogenesis in zebrafish. PLoS Biol. *4*, e10.

36. Ginsberg, M., James, D., Ding, B.S., Nolan, D., Geng, F., Butler, J.M., Schachterle, W., Pulijaal, V.R., Mathew, S., Chasen, S.T., et al. (2012). Efficient direct reprogramming of mature amniotic cells into endothelial cells by ETS factors and TGFbeta suppression. Cell *151*, 559–575.

37. Morita, R., Suzuki, M., Kasahara, H., Shimizu, N., Shichita, T., Sekiya, T., Kimura, A., Sasaki, K., Yasukawa, H., and Yoshimura, A. (2015). ETS transcription factor ETV2 directly converts human fibroblasts into functional endothelial cells. Proc. Natl. Acad. Sci. USA *112*, 160–165.

38. Veldman, M.B., Zhao, C., Gomez, G.A., Lindgren, A.G., Huang, H., Yang, H., Yao, S., Martin, B.L., Kimelman, D., and Lin, S. (2013). Transdifferentiation of fast skeletal muscle into functional endothelium in vivo by transcription factor Etv2. PLoS Biol. *11*, e1001590.

39. Swift, M.R., Pham, V.N., Castranova, D., Bell, K., Poole, R.J., and Weinstein, B.M. (2014). SoxF factors and Notch regulate nr2f2 gene expression during venous differentiation in zebrafish. Dev. Biol. *390*, 116–125.

40. Cermenati, S., Moleri, S., Cimbro, S., Corti, P., Del Giacco, L., Amodeo, R., Dejana, E., Koopman, P., Cotelli, F., and Beltrame, M. (2008). Sox18 and Sox7 play redundant roles in vascular development. Blood *111*, 2657–2666.

41. Irjala, H., Elima, K., Johansson, E.L., Merinen, M., Kontula, K., Alanen, K., Grenman, R., Salmi, M., and Jalkanen, S. (2003). The same endothelial receptor controls lymphocyte traffic both in vascular and lymphatic vessels. Eur. J. Immunol. *33*, 815–824.

42. Jung, M.Y., Park, S.Y., and Kim, I.S. (2007). Stabilin-2 is involved in lymphocyte adhesion to the hepatic sinusoidal endothelium via the interaction with alphaMbeta2 integrin. J. Leukoc. Biol. *82*, 1156–1165.

CellPress
OPEN ACCESS

43. Xia, J., Kang, Z., Xue, Y., Ding, Y., Gao, S., Zhang, Y., Lv, P., Wang, X., Ma, D., Wang, L., et al. (2021). A single-cell resolution developmental atlas of hematopoietic stem and progenitor cell expansion in zebrafish. Proc. Natl. Acad. Sci. USA *118*. e2015748118.

44. Le Mercier, A., Bonnavion, R., Yu, W., Alnouri, M.W., Ramas, S., Zhang, Y., Jäger, Y., Roquid, K.A., Jeong, H.W., Sivaraj, K.K., et al. (2021). GPR182 is an endothelium-specific atypical chemokine receptor that maintains hematopoietic stem cell homeostasis. Proc. Natl. Acad. Sci. USA *118*. e2021596118.

45. Glass, T.J., Lund, T.C., Patrinostro, X., Tolar, J., Bowman, T.V., Zon, L.I., and Blazar, B.R. (2011). Stromal cell-derived factor-1 and hematopoietic cell homing in an adult zebrafish model of hematopoietic cell transplantation. Blood *118*, 766–774.

46. Campbell, F., Bos, F.L., Sieber, S., Arias-Alpizar, G., Koch, B.E., Huwyler, J., Kros, A., and Bussmann, J. (2018). Directing nanoparticle biodistribution through evasion and exploitation of Stab2-dependent nanoparticle uptake. ACS Nano *12*, 2138–2150.

47. Baryawno, N., Przybylski, D., Kowalczyk, M.S., Kfoury, Y., Severe, N., Gustafsson, K., Kokkaliaris, K.D., Mercier, F., Tabaka, M., Hofree, M., et al. (2019). A cellular taxonomy of the bone marrow stroma in homeostasis and leukemia. Cell *177*, 1915–1932.e16.

48. Tikhonova, A.N., Dolgalev, I., Hu, H., Sivaraj, K.K., Hoxha, E., Cuesta-Domínguez, Á., Pinho, S., Akhmetzyanova, I., Gao, J., Witkowski, M., et al. (2019). The bone marrow microenvironment at single-cell resolution. Nature *569*, 222–228.

49. Khan, J.A., Mendelson, A., Kunisaki, Y., Birbrair, A., Kou, Y., Arnal-Estapé, A., Pinho, S., Ciero, P., Nakahara, F., Ma'ayan, A., et al. (2016). Fetal liver hematopoietic stem cell niches associate with portal vessels. Science *351*, 176–180.

50. Gur-Cohen, S., Yang, H., Baksh, S.C., Miao, Y., Levorse, J., Kataru, R.P., Liu, X., de la Cruz-Racelis, J., Mehrara, B.J., and Fuchs, E. (2019). Stem cell-driven lymphatic remodeling coordinates tissue regeneration. Science *366*, 1218–1225.

51. Nakahara, F., Borger, D.K., Wei, Q., Pinho, S., Maryanovich, M., Zahalka, V., Suzuki, M., Cruz, C.D., Wang, Z., Xu, C., et al. (2019). Engineering a haematopoietic stem cell niche by revitalizing mesenchymal stromal cells. Nat. Cell Biol. *21*, 560–567.

52. Chen, J., Larochelle, A., Fricker, S., Bridger, G., Dunbar, C.E., and Abkowitz, J.L. (2006). Mobilization as a preparative regimen for hematopoietic stem cell transplantation. Blood *107*, 3764–3771.

53. Chan, C.K., Chen, C.C., Luppen, C.A., Kim, J.B., DeBoer, A.T., Wei, K., Helms, J.A., Kuo, C.J., Kraft, D.L., and Weissman, I.L. (2009). Endochondral ossification is required for haematopoietic stem-cell niche formation. Nature *457*, 490–494.

54. Sacchetti, B., Funari, A., Michienzi, S., Di Cesare, S., Piersanti, S., Saggio, I., Tagliafico, E., Ferrari, S., Robey, P.G., Riminucci, M., and Bianco, P. (2007). Self-renewing osteoprogenitors in bone marrow sinusoids can organize a hematopoietic microenvironment. Cell *131*, 324–336.

55. Lin, H.F., Traver, D., Zhu, H., Dooley, K., Paw, B.H., Zon, L.I., and Handin, R.I. (2005). Analysis of thrombocyte development in CD41-GFP transgenic zebrafish. Blood *106*, 3803–3810.

56. Cross, L.M., Cook, M.A., Lin, S., Chen, J.N., and Rubinstein, A.L. (2003). Rapid analysis of angiogenesis drugs in a live fluorescent zebrafish assay. Arterioscler. Thromb. Vasc. Biol. *23*, 911–912.

57. Chi, N.C., Shaw, R.M., De Val, S., Kang, G., Jan, L.Y., Black, B.L., and Stainier, D.Y. (2008). Foxn4 directly regulates tbx2b expression and atrioventricular canal formation. Genes Dev. *22*, 734–739.

58. Ellett, F., Pase, L., Hayman, J.W., Andrianopoulos, A., and Lieschke, G.J. (2011). mpeg1 promoter transgenes direct macrophage-lineage expression in zebrafish. Blood *117*, e49–e56.

59. Zilionis, R., Nainys, J., Veres, A., Savova, V., Zemmour, D., Klein, A.M., and Mazutis, L. (2017). Single-cell barcoding and sequencing using droplet microfluidics. Nat. Protoc. *12*, 44–73.

60. Buenrostro, J.D., Giresi, P.G., Zaba, L.C., Chang, H.Y., and Greenleaf, W.J. (2013). Transposition of native chromatin for fast and sensitive epigenomic profiling of open chromatin, DNA-binding proteins and nucleosome position. Nat. Methods *10*, 1213–1218.

61. Trapnell, C., Pachter, L., and Salzberg, S.L. (2009). TopHat: discovering splice junctions with RNA-Seq. Bioinformatics *25*, 1105–1111.

62. Trapnell, C., Williams, B.A., Pertea, G., Mortazavi, A., Kwan, G., van Baren, M.J., Salzberg, S.L., Wold, B.J., and Pachter, L. (2010). Transcript assembly and quantification by RNA-Seq reveals unannotated transcripts and isoform switching during cell differentiation. Nat. Biotechnol. *28*, 511–515.

63. Langmead, B., and Salzberg, S.L. (2012). Fast gapped-read alignment with Bowtie 2. Nat. Methods *9*, 357–359.

64. Zhang, Y., Liu, T., Meyer, C.A., Eeckhoute, J., Johnson, D.S., Bernstein, B.E., Nusbaum, C., Myers, R.M., Brown, M., Li, W., and Liu, X.S. (2008). Model-based analysis of ChIP-Seq (MACS). Genome Biol. *9*, R137.

65. Heinz, S., Benner, C., Spann, N., Bertolino, E., Lin, Y.C., Laslo, P., Cheng, J.X., Murre, C., Singh, H., and Glass, C.K. (2010). Simple combinations of lineage-determining transcription factors prime cis-regulatory elements required for macrophage and B cell identities. Mol. Cell *38*, 576–589.

66. Sandelin, A., Wasserman, W.W., and Lenhard, B. (2004). ConSite: web-based prediction of regulatory elements using cross-species comparison. Nucleic Acids Res. *32*, W249–W252.

67. Tang, Q., Iyer, S., Lobbardi, R., Moore, J.C., Chen, H., Lareau, C., Hebert, C., Shaw, M.L., Neftel, C., Suva, M.L., et al. (2017). Dissecting hematopoietic and renal cell heterogeneity in adult zebrafish at single-cell resolution using RNA sequencing. J. Exp. Med. *214*, 2875–2887.

68. Thisse, C., and Thisse, B. (2008). High-resolution in situ hybridization to whole-mount zebrafish embryos. Nat. Protoc. *3*, 59–69.

69. Mosimann, C., Kaufman, C.K., Li, P., Pugach, E.K., Tamplin, O.J., and Zon, L.I. (2011). Ubiquitous transgene expression and Cre-based recombination driven by the ubiquitin promoter in zebrafish. Development *138*, 169–177.

70. Adám, A., Bártfai, R., Lele, Z., Krone, P.H., and Orbán, L. (2000). Heat-inducible expression of a reporter gene detected by transient assay in zebrafish. Exp. Cell Res. *256*, 282–290.

71. Ju, B., Chong, S.W., He, J., Wang, X., Xu, Y., Wan, H., Tong, Y., Yan, T., Korzh, V., and Gong, Z. (2003). Recapitulation of fast skeletal muscle development in zebrafish by transgenic expression of GFP under the mylz2 promoter. Dev. Dyn. *227*, 14–26.

72. Chen, J., Carney, S.A., Peterson, R.E., and Heideman, W. (2008). Comparative genomics identifies genes mediating cardiotoxicity in the embryonic zebrafish heart. Physiol. Genomics *33*, 148–158.

73. Wu, B.J., Chiu, C.C., Chen, C.L., Wang, W.D., Wang, J.H., Wen, Z.H., Liu, W., Chang, H.W., and Wu, C.Y. (2014). Nuclear receptor subfamily 2 group F member 1a (nr2f1a) is required for vascular development in zebrafish. PLoS One *9*, e105939.

74. Dinh, T.T., Girke, T., Liu, X., Yant, L., Schmid, M., and Chen, X. (2012). The floral homeotic protein APETALA2 recognizes and acts through an AT-rich sequence element. Development *139*, 1978–1986.

STAR★METHODS

KEY RESOURCES TABLE

REAGENT or RESOURCE	SOURCE	IDENTIFIER
Antibodies		
Anti-NR2F2	R&D Biosystems	Cat#PP-H7147-00; RRID: 2155627
Chemicals, peptides, and recombinant proteins		
Liberase TM Research Grade	Millipore Sigma	Cat# 5401119001
Klenow fragment	NEB	Cat# M0210S
GenElute LPA	Sigma	Cat# 56575
TRIzol LS Reagent	ThermoFisher	Cat# 10296010
Leica Tissue Freezing Medium	Leica	Cat# 14020108926
Tissue-Tek Cryomolds	VWR	https://us.vwr.com/store/product/4639407/tissue-tek-cryomold-molds-adapters-sakura-finetek
Critical commercial assays		
SMARTer Universal Low Input RNA Kit	Takara Clontech	Cat# 634938
pENTR 5'-TOPO TA Cloning Kit	ThermoFisher	Cat# K59120
Deposited data		
Zebrafish tomo-seq, RNA-seq and ATAC-seq data	This paper	GEO: GSE124151
Mouse endothelial bulk RNA-seq data	Barry et al.[30]	GEO: GSE129005
Adult zebrafish kidney marrow scRNA-seq	Tang et al.[67]	https://molpath.shinyapps.io/zebrafishblood/
Experimental models: Organisms/strains		
Zebrafish: Tg(mrc1a 1.3 kb:GFP)	This paper	N/A
Zebrafish: Tg(sele 5.3 kb:GFP)	This paper	N/A
Zebrafish: Tg(mrc1a 125 bp:GFP)	This paper	N/A
Zebrafish: Tg(sele 158 bp:GFP)	This paper	N/A
Zebrafish: Tg(stab2 422 bp:GFP)	This paper	N/A
Zebrafish: Tg(nrp1b 552 bp:GFP)	This paper	N/A
Zebrafish: Tg(cdh5 823 bp:GFP)	This paper	N/A
Oligonucleotides		
Primers use for WISH probe synthesis	This paper	See Table S8
Primers used to clone promoter and enhancer elements	This paper	See Table S9
Sequences and primers used for enhancer variants	This paper	See Table S10
Primers used for cloning and EMSA probe synthesis	This paper	See Table S11
Morpholino: sox7-ATG MO: 5'- ACGC ACTTATCAGAGCCGCCATGTG - 3'	Swift et al.[39]	https://www.gene-tools.com/
Morpholino: sox18-ATG MO: 5' –TATT CATTCCAGCAAGACCAACACG - 3'	Swift et al.[39]	https://www.gene-tools.com/
Morpholino: nr2f1a-ATG MO: 5'-CCAG ACGCTAACTACCATTGCCATA - 3'	Wu et al.[73]	https://www.gene-tools.com/
Morpholino: nr2f2-ATG MO: 5' – AGCC TCTCCACACTACCATTGCCAT – 3'	Swift et al.[39]	https://www.gene-tools.com/
Morpholino: nr2f5-ATG MO: 5'-CACTG ATTTACTACCATTGCCATGC - 3'	Chen et al.[72]	https://www.gene-tools.com/
Morpholino: Standard Control MO: 5' - CCTCTTACCTCAGTTACAATTTATA - 3'	Gene Tools	https://www.gene-tools.com/

(*Continued on next page*)

CellPress
OPEN ACCESS

Continued

REAGENT or RESOURCE	SOURCE	IDENTIFIER
Software and algorithms		
Imaris	Oxford Instruments	https://imaris.oxinst.com/
Elements	Nikon	https://www.microscope.healthcare.nikon.com/products/software/nis-elements
HOMER	Heinz et al.[65]	http://homer.ucsd.edu/homer/motif/
MACS2	Zhang et al.[64]	https://github.com/macs3-project/MACS
Consite	Sandelin et al.[66]	http://www.phylofoot.org/consite.
Bowtie2 (version 2.2.1)	Langmead and Salzberg[63]	https://bowtie-bio.sourceforge.net/bowtie2/manual.shtml
Cufflinks 2.2.1	Trapnell et al.[62]	http://cole-trapnell-lab.github.io/cufflinks/manual/
Tophat 2.0.11	Trapnell et al.[61]	https://ccb.jhu.edu/software/tophat/index.shtml
GraphPad Prism v.7.03	GraphPad	https://www.graphpad.com/features

RESOURCE AVAILABILITY

Lead contact

Further information and requests for resources and reagents should be directed to and will be fulfilled by the lead contact, Leonard Zon (zon@enders.tch.harvard.edu)

Materials availability

Plasmids generated in this study will be shared by the lead contact upon request.

Transgenic zebrafish lines generated in this study will be shared by the lead contact upon request.

Data and code availability

- All tomo-seq, bulk RNA-seq, single cell RNA-seq and ATAC-seq data have been deposited at GEO and are publicly available as of the date of publication. Accession numbers are listed in the key resources table. Microscopy data reported in this paper will be shared by the lead contact upon request.
- This paper does not report original code.
- Any additional information required to reanalyze the data reported in this paper is available from the lead contact upon request.

EXPERIMENTAL MODEL AND SUBJECT DETAILS

Animals

Wild-type AB, *casper* or *casper*-EKK, and transgenic zebrafish (*Danio rerio*) lines *cd41:EGFP*,[55] *runx1:mCherry* [*runx1+23:NLS-mCherry*],[17] *kdrl(flk1):GFP* [*kdrl:GRCFP*],[56] *kdrl:mCherry* [*kdrl:Hsa.hras-mCherry*],[57] *cxcl12a(sdf1a):DsRed2*,[45] and *mpeg1:mCherry*[58] were used in this study. Alternative gene names are listed in parenthesis and full transgene names are listed in brackets. All zebrafish were housed at Boston Children's Hospital and handled according to approved Institutional Animal Care and Use Committee (IACUC) of Boston Children's Hospital protocols. Zebrafish (*Danio rerio*) stocks were maintained at 28C in a recirculating system and bred by putting male-female pairs into a mating tank and controlling the day-night cycle. Male and female breeders from 3-9 months of age were used to generate fish for all experiments. Analyses of the adult kidney marrow was performed using 3-6 month old fish. No tests on the influence of sex were preformed in this study; sex determination in zebrafish occurs in late juvenile stage.

METHOD DETAILS

Genomic analyses

For RNA tomography (tomo-seq), 72 hpf embryos were euthanized by tricaine overdose and the portion of the tail containing the CHT was manually dissected using a scalpel. The tissue was oriented in OCT tissue freezing media (Leica) in a cryomold (Tissue-TEK) with the ventral side facing the bottom of the mold. After snap freezing on dry ice, 40 individual 8 μm-thick cryosections were collected along the dorsal-ventral axis using a cryostat. The RNA from individual cryosections was extracted using TRIzol and then barcoded during a reverse transcription step prior to pooling for library preparation and sequencing.[27] For inDrops single cell and bulk RNA-seq, *kdrl*:GFP embryos were dissociated using Liberase (Roche) and GFP^+ cells were isolated by FACS. For bulk RNA-seq, total RNA was isolated using TRIzol LS and GenElute LPA (Sigma) carrier as per manufacturer's instructions. Libraries were prepared from 50 ng of total RNA/sample as input using Ribogone and a SMARTer Universal Low Input RNA Kit (Clontech). For inDrops, approximately 2,000 cells were encapsulated and libraries were prepared for sequencing.[59] For ATAC-seq, embryos were dissociated using

Liberase and a minimum of 12,000 cells (max 50,000) were isolated by FACS. Cells were subsequently lysed and isolated nuclei were incubated in a transposition reaction.[60] All sequencing was done using an Illumina Hiseq 2500. For RNA-seq, quality control was performed by Fast QC and Cutadapt to remove adaptor sequences and low quality regions. High-quality reads were aligned to UCSC build danRer7 of the zebrafish genome using Tophat 2.0.11[61] without novel splicing form calls. Transcript abundance and differential expression were calculated with Cufflinks 2.2.1.[62] FPKM values were used to normalize and quantify each transcript. For ATAC-seq, reads were aligned to UCSC build danRer7 of the zebrafish genome using Bowtie2 (version 2.2.1)[63] with the following parameters: –end-to-end, -N0-, -L20. The MACS2 (version 2.1.0) peak finding algorithm[64] was used to identify regions of ATAC-seq peaks with the following parameters: –nomodel –shift -100 –extsize 200. An initial q-value threshold of enrichment of 0.05 was used for peak calling and a more stringent q-value of 14 was used to identify peaks that were distinct between different samples. Genome-wide motif enrichment analysis was performed using HOMER[65] and motif annotation was done using Consite.[66] Gene expression analysis of the adult kidney marrow was performed using publicly available data (https://molpath.shinyapps.io/zebrafishblood/).[67]

Whole mount *in situ* hybridization (WISH)

In situ hybridization was performed using a standard *in situ* protocol.[68] Embryos were subsequently transferred to glycerol for scoring and imaging. *In situ* probes were generated by PCR amplification using a cDNA or plasmid (for transcription factors from other species) template followed by reverse transcription with digoxigenin-linked nucleotides. Primer sequences for all WISH probes used in this paper are provided in Table S8.

Transgenesis and enhancer-GFP reporter assays

Transgenic lines were established a standard Tol2 protocol.[69] For the *mrc1a 1.3kb*:GFP and *sele 5.3kb*:GFP transgenes, 1.3 kb and 5.3 kb sequences, respectively, upstream of the transcriptional start site were PCR amplified off of genomic DNA and then TOPO-TA cloned into a p5E Gateway vector (Invitrogen), which was then recombined with GFP and a polyA tail, all flanked by Tol2 sites. For the 125 bp *mrc1a* and 158 bp *sele* enhancers, the elements were PCR amplified off of genomic DNA, TOPO-TA cloned into a p5E Gateway vector and then recombined with the mouse *Beta-globin* minimal promoter[17] fused to GFP with a polyA tail, all flanked by Tol2 sites. Embryos were injected at the one cell-stage with Tol2 RNA and at least two independent lines showing similar expression were established for each construct: (Tg(*mrc1a 1.3kb*:GFP); Tg(*sele 5.3kb*:GFP); Tg(*mrc1a 125bp*:GFP); and Tg(*sele 158bp*:GFP). The CHT EC and pan-EC ATAC-seq elements were similarly amplified by PCR using genomic DNA and then fused to the *Beta-globin* minimal promoter and GFP. Mutational variants of 125 bp *mrc1a* and 158 bp *sele* were generated by annealing overlapping oligos followed by a T4 DNA polymerase reaction to generate blunt-ended products, which were subsequently cloned into p5E Gateway vectors (following A-tailing with Klenow Fragment (NEB)) using the same work flow as for the ATAC-seq elements. Transcription factor binding motifs were disrupted by changing nucleotides in the core binding sites, purines for pyrimidines and vice versa. Injected F0 embryos were scored between 60-72 hpf, and embryos were scored as positive if there were GFP+ ECs present in the CHT. Control and experimental groups were blinded prior to scoring and all experiments were performed at least three times, with independent clutches. GFP expression in CHT ECs or pan-EC expression was scored as significant if it was observed in at least 10% of F0 injected embryos. Embryos scored as negative had either no GFP expression or had only sparse ectopic expression in muscle cells. The sequences for primers used to amplify the *mrc1a* and *sele* regulatory elements, as well as the 15 CHT EC and 6 pan-EC ATAC-seq elements, are provided in Table S9. The sequences for the overlapping oligos that were used to generate the enhancer variants are provided in Table S10. The fidelity of all constructs was confirmed by sequencing prior to injection.

Transcription factor overexpression studies

For transcription factor overexpression studies, the open reading frames for the human (FLI1, ETV2, ETS1, SOX7 and RXRA), xenopus (Sox18) or zebrafish (Nr2f2) genes were cloned into a pME Gateway vector (Invitrogen) and then recombined with the zebrafish *ubi* promoter,[69] *hsp70l* promoter,[70] *nrp1b* enhancer, or *mylz2* promoter,[71] and a polyA tail, all flanked by Tol2 sites. The fidelity of all constructs was confirmed by sequencing prior to injection. Embryos were injected with transcription factor pools (1 nl at 25 ng/μl total DNA, plus Tol2 RNA) at the one cell-stage and then screened between 24-72 hpf for ectopic niche endothelial gene expression or ectopic HSPC localization. For control and single-factor injections, the empty Tol2 Gateway destination vector was used as filler DNA in the injection mix. Expression of the transcription factors was confirmed by WISH using species-specific *in situ* probes. Ectopic expression was scored as vascular staining or vascular GFP expression outside the normal domain of gene expression.

Microscopy and image analysis

Time-lapse microscopy was performed using a Yokogawa CSU-X1 spinning disk mounted on an inverted Nikon Eclipse Ti microscope equipped with dual Andor iXon EMCCD cameras and a climate controlled (maintained at 28.5C) motorized x-y stage to facilitate tiling and imaging of multiple specimens simultaneously. Screening of injected enhancer-GFP constructs and imaging of WISH embryos was performed using a Nikon SMZ18 stereomicroscope equipped with a Nikon DS-Ri2 camera. All images were acquired using NIS-Elements (Nikon) and processed using Imaris (Oxford Instruments) or Adobe Photoshop software. HSPC dynamics were quantified using Imaris and vessel morphology was analyzed using the AngioTool software package in Fiji. Embryos were mounted for imaging in 0.8% LMP agarose with tricaine (0.16 mg/ml) in glass bottom 6-well plates and covered with E3 media containing tricaine (0.16 mg/ml).[17]

CellPress
OPEN ACCESS

Flow cytometry, kidney marrow dissection, dissociation, and histology

Embryos were prepared for FACS by chopping with a razor blade in cold PBS and then incubating in Liberase (Roche) for 20 min at 37C before filtering the dissociated cells through a 40 μm mesh filter and transferring to 2% FBS.[17] FACS was performed using a FACS Aria machine (BD Biosciences). Gates were set to select the brightest cells, using transgene positive and negative control samples as a guide and SYTOX Blue as a live/dead stain. Single cell RNA-seq analysis of FACS-sorted *kdrl:GFP*+ cells was used to supplement bulk RNA-seq to distinguish genes that were expressed by myeloid versus endothelial cells. At least 12,000 (50,000 max) cells were collected per sample for ATAC-seq experiments and at least 10,000 (300,000 max) cells per sample were collected for RNA-seq experiments. Kidney marrow was harvested from adult zebrafish by manual dissection and then dissociated using Liberase or fixed in 4% PFA (for histology) or dissociated by gentle pipetting (for live cell imaging). For histology the kidney marrow was embedded in paraffin prior to sectioning; alternating sections were stained with H&E or with an antibody to GFP. Mouse EC populations were sorted as $Cd45^{-}Pdpn^{-}Cd31^{+}$ cells.[30]

Morpholino injections

Morpholinos (MOs, Gene Tools) were diluted in water with phenol red and injected into 1- to 2-cell stage embryos.[39,72,73] For the Nr2f MO injections, each MO was injected at a one third dose.

Electrophoretic mobility shift assay

The Nr2f2 fragment was cloned into the pGEX2TK vector (GE Healthcare) to generate GST-tagged Nr2f2 and fidelity was verified by sequencing. The pGEX2TK-Nr2f2 protein plasmid was transformed into *E. coli* BL21 competent cells. Protein expression and purification were carried out as previously described[74] and purified proteins were quantified against BSA. EMSAs were performed as previously described.[74] Probes were generated by annealing 100 pmol of sense and antisense oligonucleotides and 1-2 pmol of probe was used in each reaction. All primer and probe sequences are provided in Table S11. Gel shift reactions were conducted at 4°C in 20% glycerol, 20 mM Tris (pH 8.0), 10 mM KCl, 1 mM DTT, 12.5 ng poly dI/C, 6.25 pmol of random, single-stranded oligonucleotides, BSA and the probe in the amount specified above. Samples involving the Nr2f2 protein were loaded on a 6% gel to resolve protein-DNA complexes. In reactions with cold competitors, 20x unlabeled probes were included in the reactions. Anti-NR2F2 (R&D Biosystems; cat # PP-H7147-00) was at the same amount of the Nr2f2 protein to obtain super-shifts.

QUANTIFICATION AND STATISTICAL ANALYSIS

For all graphs, error bars report mean ± s.e.m. One-way ANOVA analyses were followed by Dunnett's (enhancer variant analyses) or Tukey's (vessel analyses and HSPC budding) post hoc tests for multiple comparisons. Chi Square Test was used for comparing mrc1a 125bp:GFP expression data. To compare transcription factor injections, Chi Square Test and Fisher's exact tests were used, with the Holm step-down process to correct for multiple comparisons. Unpaired two-tailed Student's t-test or two-tailed Mann-Whitney tests were used to analyze HSPC counts and HSPC residency time, respectively. Data were analyzed using GraphPad Prism v.7.03, $P < 0.05$ was considered to be statistically significant. At least three independent biological replicates were performed for each experiment, with at least 15 animals from randomized, independent groups to ensure sufficient sample sized for statistical analysis. Control and experimental samples were blinded prior to scoring and all experiments were performed at least three times, with independent clutches. No data was excluded from any of the analyses.

Developmental Cell, Volume *58*

Supplemental information

Transcription factor induction

of vascular blood stem cell niches *in vivo*

Elliott J. Hagedorn, Julie R. Perlin, Rebecca J. Freeman, Samuel J. Wattrus, Tianxiao Han, Clara Mao, Ji Wook Kim, Inés Fernández-Maestre, Madeleine L. Daily, Christopher D'Amato, Michael J. Fairchild, Raquel Riquelme, Brian Li, Dana A.V.E. Ragoonanan, Khaliun Enkhbayar, Emily L. Henault, Helen G. Wang, Shelby E. Redfield, Samantha H. Collins, Asher Lichtig, Song Yang, Yi Zhou, Balvir Kunar, Jesus Maria Gomez-Salinero, Thanh T. Dinh, Junliang Pan, Karoline Holler, Henry A. Feldman, Eugene C. Butcher, Alexander van Oudenaarden, Shahin Rafii, J. Philipp Junker, and Leonard I. Zon

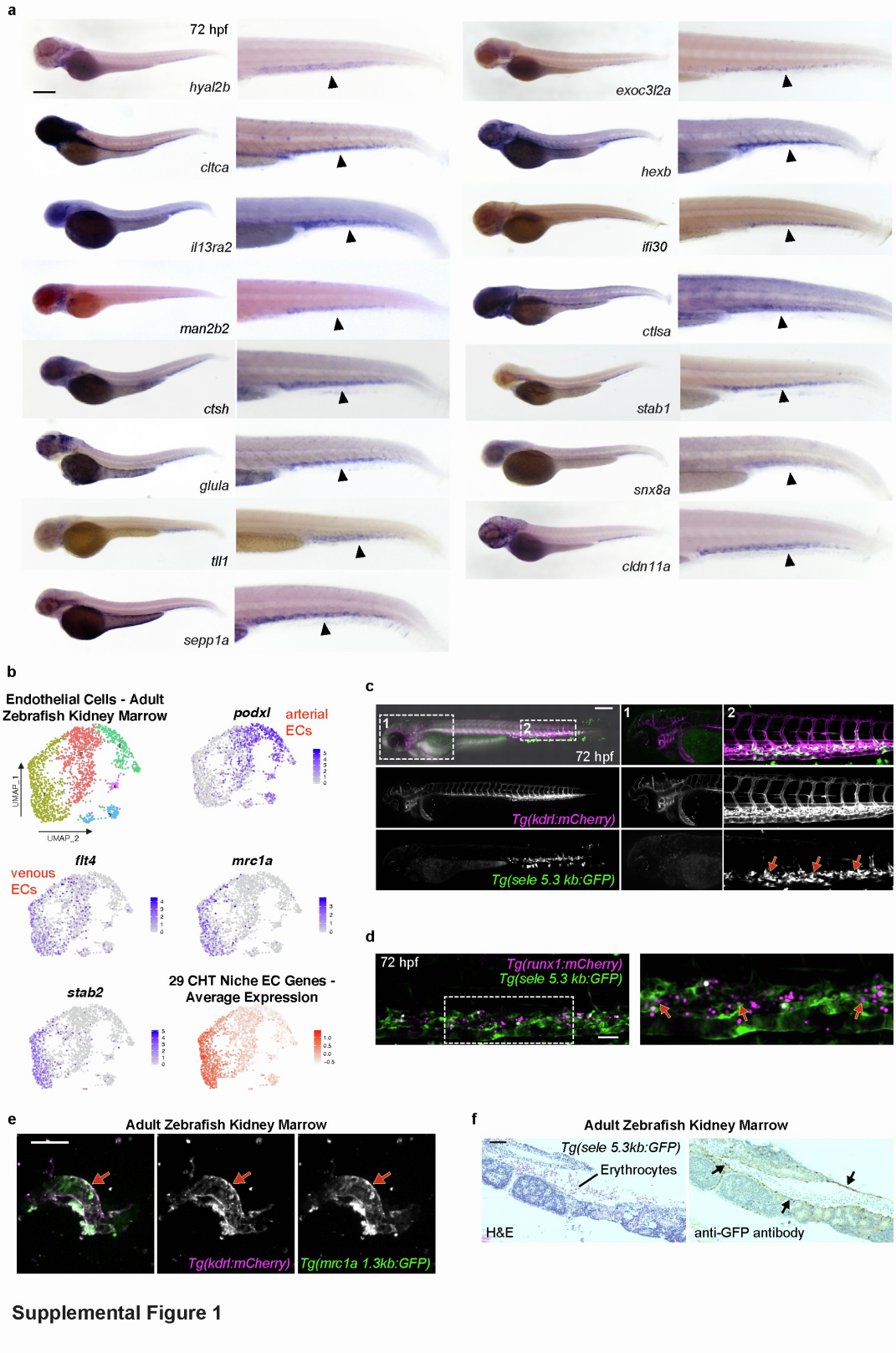

Supplemental Figure 1

Supplemental Figure 1 | Niche-specific endothelial gene expression (related to Figures 1 and 2). **a**, WISH validates the CHT-enriched expression (arrowheads) of CHT EC genes identified using a combination of tomo-seq and tissue-specific RNA-seq. Scale bars represent 250 μm in this and all subsequent Supplemental Figures unless noted otherwise. **b**, Uniform Manifold Approximation and Projection (UMAP) plots show cell clustering and gene expression from a single cell RNA-seq analysis of *kdrl:mCherry*$^{+}$ endothelial cells isolated from adult zebrafish kidney marrow. Marker genes are shown for arterial (*podxl*) and venous (*flt4*) endothelial cells, as well as CHT ECs (*mrc1a* and *stab2*). The average expression of the 29 CHT niche EC genes is shown in the bottom right plot. Spectral scales report z-scores. **c**, Images show a double transgenic embryo carrying the pan-endothelial marker *kdrl:mCherry* (magenta) and the *sele 5.3kb:GFP* transgene (green). Magnifications of boxed areas are shown on the right. The highest levels of vascular GFP expression are observed in CHT ECs (red arrows); while lower levels of expression are observed in the anterior head region, although some of these cells do not express the *kdrl:mCherry* transgene. **d**, Images show *runx1:mCherry*$^{+}$ HSPCs (magenta) directly interacting with *sele 5.3kb:GFP*$^{+}$ ECs within the CHT niche (red arrows). Panel on right shows magnification of boxed area. **e**, Images show a segment of vasculature (red arrows) dissected from the kidney of a *mrc1a 1.3kb:GFP; kdrl:mCherry* double transgenic adult zebrafish. **f**, Images show sequential sections through an adult kidney isolated from a *sele 5.3kb:GFP* transgenic fish. Sections were stained with H&E (left) and with an antibody against GFP (right). Black arrows point to GFP^{+} vascular endothelial cells. Scale bars represent 50 μm in **d-f**.

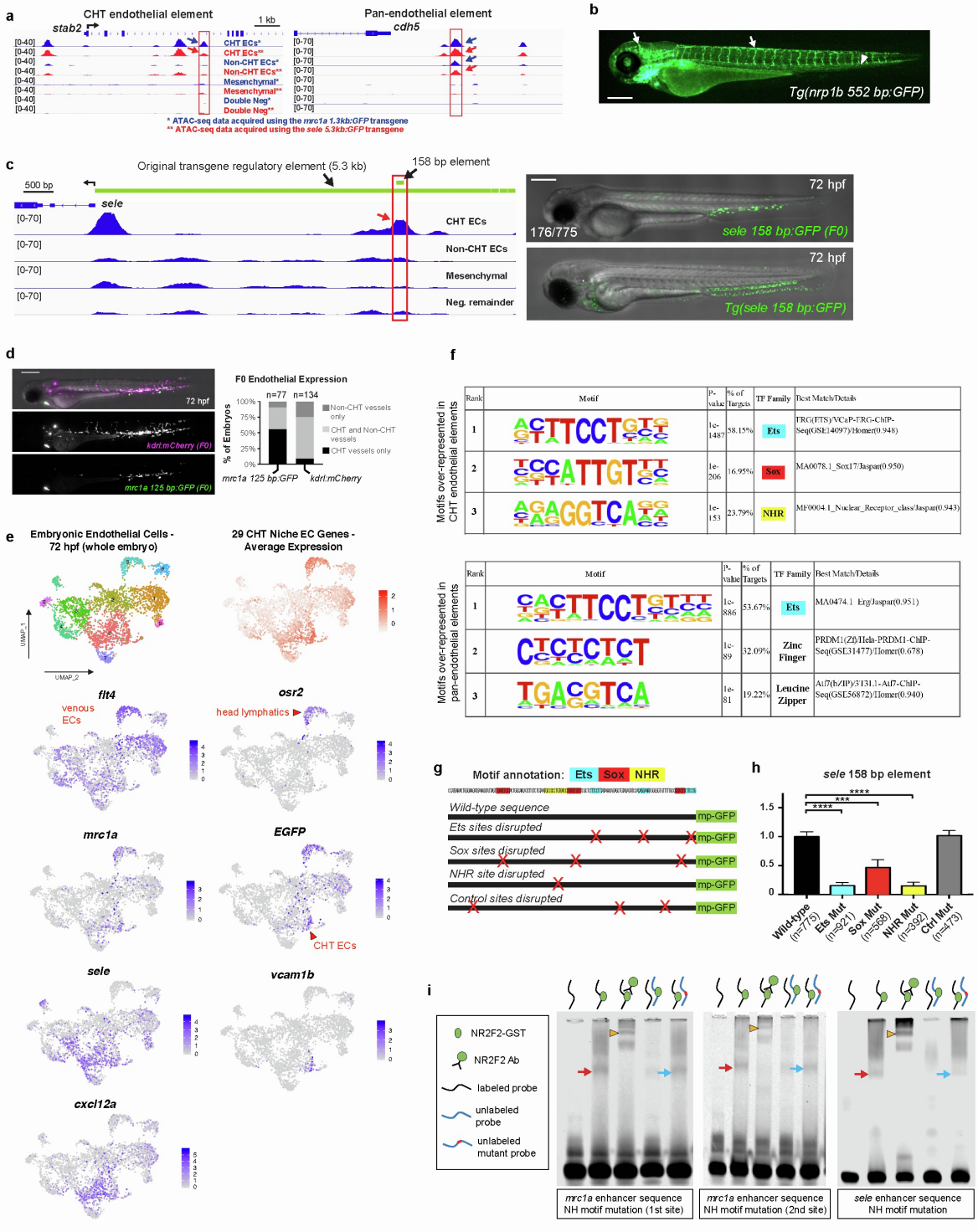

Supplemental Figure 2

Supplemental Figure 2 | A *cis*-regulatory landscape for HSPC niche- and pan-endothelial gene expression (related to Figures 3 and 4). **a**, Gene tracks show regions of chromatin that were uniquely open in the mCherry^{+}; GFP^{+} CHT EC fraction (left; red box and arrows) or a region of chromatin open in both the mCherry^{+}GFP^{+} (CHT EC) and mCherry^{+}GFP^{-} (non-CHT EC) populations (right; red box and arrows). The blue tracks show ATAC-seq data obtained using the *mrc1a 1.3kb:GFP* transgene, while the red tracks show ATAC-seq data obtained using the *sele 5.3kb:GFP* transgene. **b**, Image shows reporter expression for the stable *nrp1b:552bp:GFP* enhancer transgene. Arrows point to GFP expression in non-CHT ECs and arrowhead points to expression in CHT ECs. **c**, Gene tracks show a region of chromatin upstream of *sele* that was uniquely open in the double positive CHT EC fraction but not the other three cell populations (red box and arrow). Green bars denote the position of the 158 bp enhancer sequence and the 5.3 kb sequence used to generate the *sele:GFP* reporter transgenes. Images show transient F0 (upper right) and stably integrated (lower right) transgene expression of the *sele 158 bp:GFP* construct. **d**, Images show an F0 embryo injected with *mrc1a 125 bp:GFP* and *kdrl:mCherry* plasmids. Graph reports the anatomical location of endothelial expression in F0 embryos that were injected with each construct. **e**, Uniform Manifold Approximation and Projection (UMAP) plots show cell clustering and gene expression from a single cell RNA-seq analysis of endothelial cells (whole embryo) isolated from *mrc1a 125bp:GFP*; *kdrl:mCherry* double positive embryos at 72 hpf. *osr2* expression is shown as a marker of the head lymphatic EC population. Spectral scales report z-scores. **f**, Tables show the transcription factor binding motifs most enriched in CHT EC regions (top) or pan-endothelial regions (bottom). **g**, Wild-type sequence of the 158 bp *sele*

enhancer is shown, annotated with colors highlighting the Ets, Sox and NHR binding motifs (top). Schematic depicts sequence variants in which each class of motif or control regions were targeted by mutation. Red X's denote the location of targeted sites. mp-GFP: mouse *Beta-globin* minimal promoter fused to GFP. **h**, Graph reports the frequency of embryos with GFP expression in CHT ECs after injection with wild-type sequences or mutated variants of the *sele* 158 bp enhancer. Data is normalized to the wild-type control (23% GFP^+ CHT ECs (176/775)). Mean +/- s.e.m., One-way ANOVA with Dunnett's multiple comparisons test; ***P<0.001, ****P<0.0001. **i**, Images show electrophoretic mobility shift assays with recombinant Nr2f2-GST that was incubated with DNA sequences spanning the NHR motifs present in the 125 bp *mrc1a* (left two gels) or 158 bp *sele* (right gel) enhancer sequences. Red arrows point to DNA:protein binding while orange arrowheads point to super-shifted DNA:protein complexes. Labeled DNA:protein complexes were outcompeted by unlabeled wild-type probe (lane 4) but not by unlabeled probe in which the NHR motif was disrupted by mutation (blue arrows). All experiments were performed at least three times, with independent clutches.

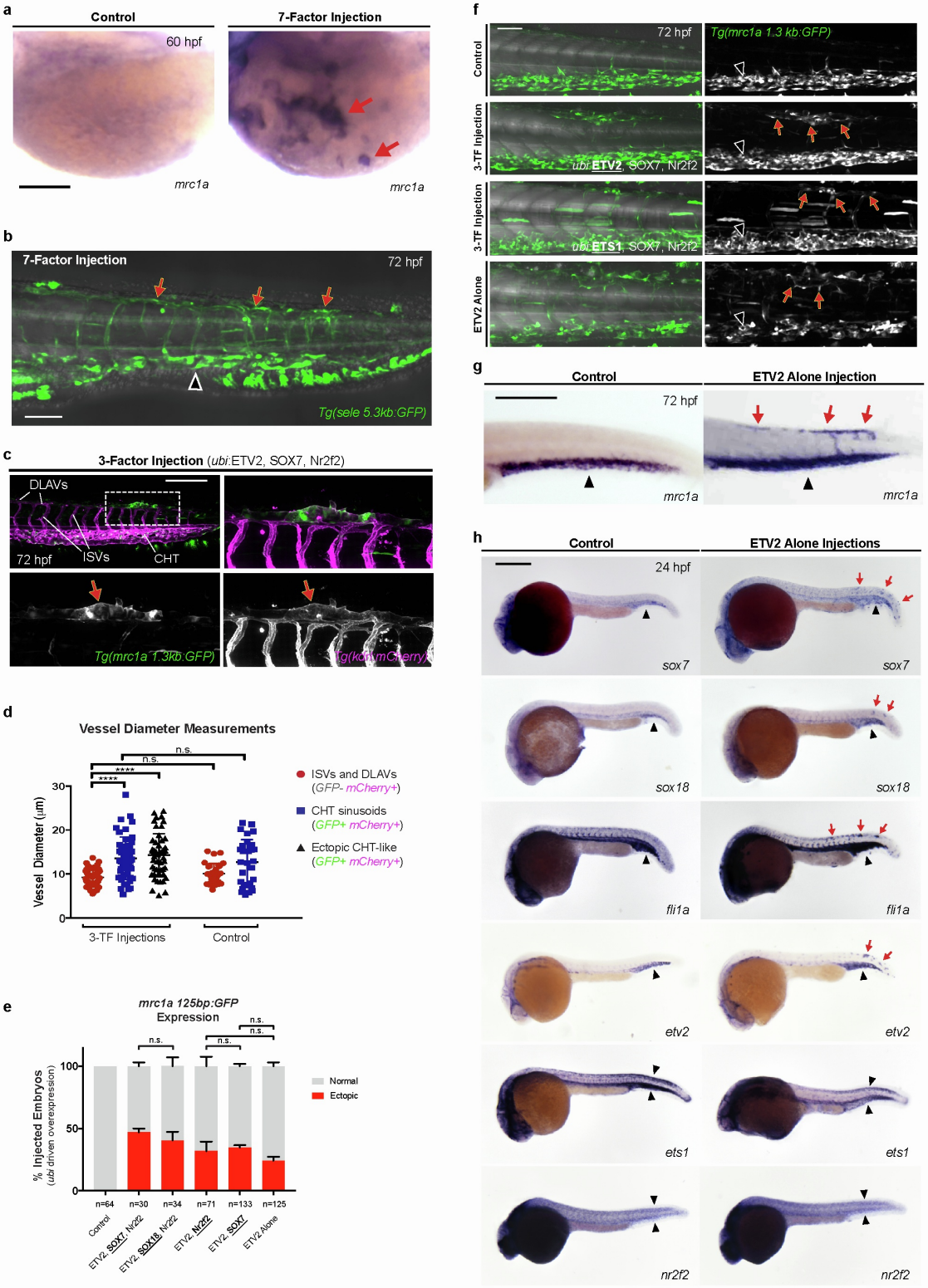

Supplemental Figure 3

Supplemental Figure 3 | Transcription factor induction of niche EC gene expression (related to Figure 5 and 6). a, Images show WISH staining for *mrc1a* over the yolk ball in a control (left) and 7-factor injected embryo (right). **b**, Image shows a *sele 5.3kb:GFP* transgenic embryo that was injected with the 7-factor pool. **c**, Images show a large vessel in the dorsal tail region (red arrow) ectopically expressing *mrc1a 125bp:GFP* (green) and *kdrl:mCherry* (magenta). Magnification of white dotted box is shown on the right. Dorsal longitudinal anastomotic vessels (DLAVs); Intersegmental vessels (ISVs). **d**, Graph reports quantitative measurements of vessel diameter for intersegmental vessels (ISVs) and dorsal longitudinal anastomotic vessels (DLAVs), and CHT sinusoidal vessels in *ubi*:ETV2, SOX7 and N2f2 and control injected embryos. One-way ANOVA with Tukey's test for multiple comparisons; ****P<0.0001; n.s. = not significant. **e**, Graph reports the percentage of transcription factor-injected embryos that showed ectopic expression of *mrc1a 125bp:GFP.* Fisher's exact test for pairwise comparisons was used; n.s. = not significant. **e**, Graph reports the percentage of transcription factor-injected embryos that showed ectopic expression of *mrc1a 125bp:GFP.* Fisher's exact test for pairwise comparisons was used; n.s. = not significant. **f**, Images show *mrc1a 1.3kb:GFP* transgenic embryos that were injected with different combinations of transcription factors at the one-cell stage. Grayscale images of the GFP signal are shown on the right. Red arrows denote regions of ectopic expression and black arrowheads point to normal domains of expression in all panels of this figure. **g-h**, Injection of human ETV2 alone induces ectopic expression of *mrc1a* (**g**) and zebrafish transcription factors (**h**), including *sox7*, *sox18*, *fli1a* and *etv2*. Embryos shown range from 24-36 hpf. All experiments were

performed at least three times, with independent clutches. Scale bar represents 100 μm in **a**-**c** and **f**.

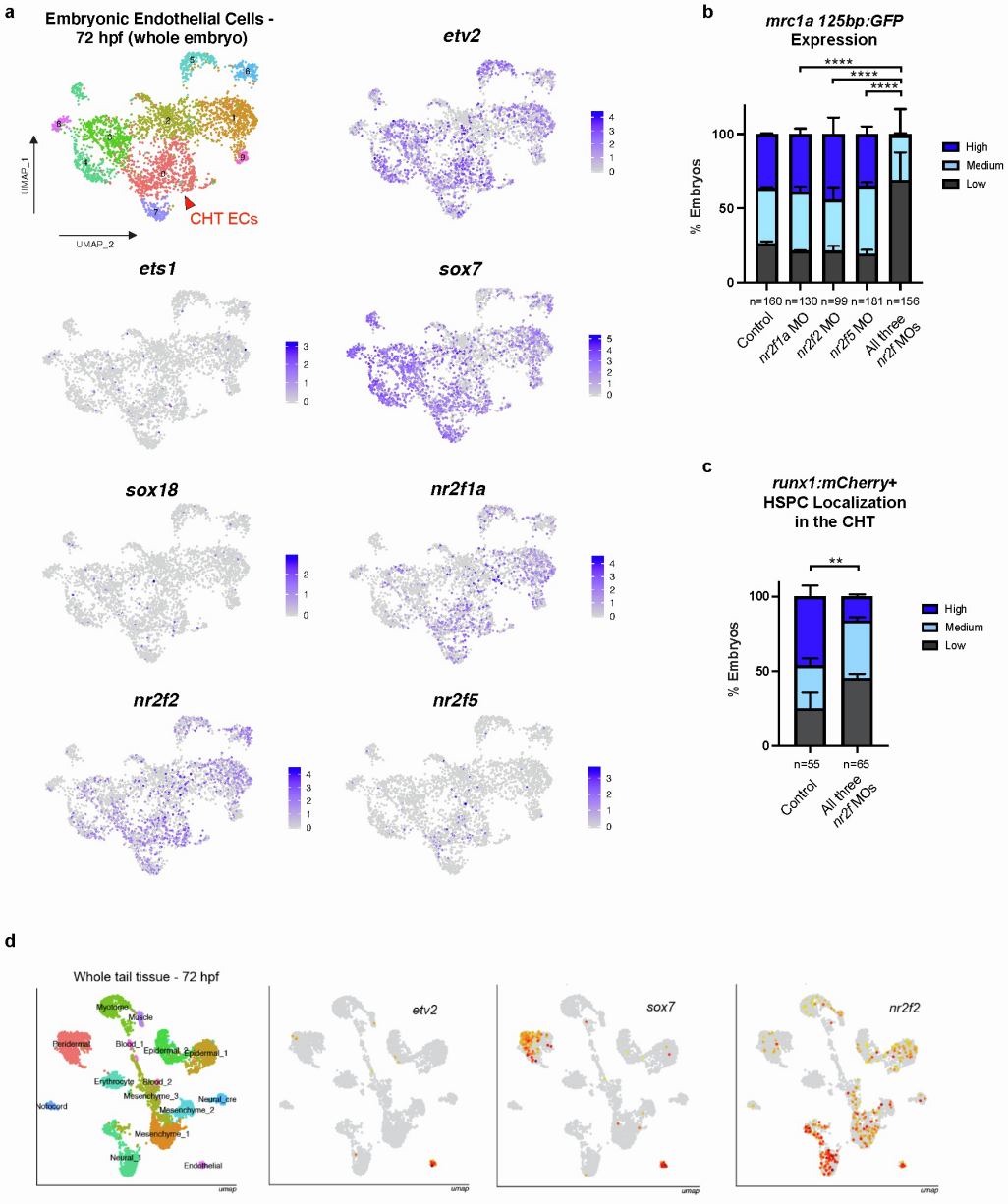

Supplemental Figure 4

Supplemental Figure 4 | Redundancy in the transcription factor regulation of niche EC gene expression (related to Figure 6). **a**, Uniform Manifold Approximation and Projection (UMAP) plots show cell clustering and gene expression from a single cell RNA-seq analysis of endothelial cells isolated from embryos at 72 hpf. Spectral scales report z-scores. **b-c,** Bar graphs report the quantification of *mrc1a 125bp:GFP* expression (**b**) and HSPC localization (**c**) in animals injected with the *nr2f1a, nr2f2, nr2f5* or control morpholinos. Chi squared test; **P<0.01,****P<0.0001. **d**, UMAP plots show single cell RNA-seq data on whole tail tissue dissected from 72 hpf embryos. The plot on the left includes labels for the distinct cell populations. The remaining three plots show the expression for *etv2*, *sox7* and *nr2f2*. All experiments were performed at least three times, with independent clutches.

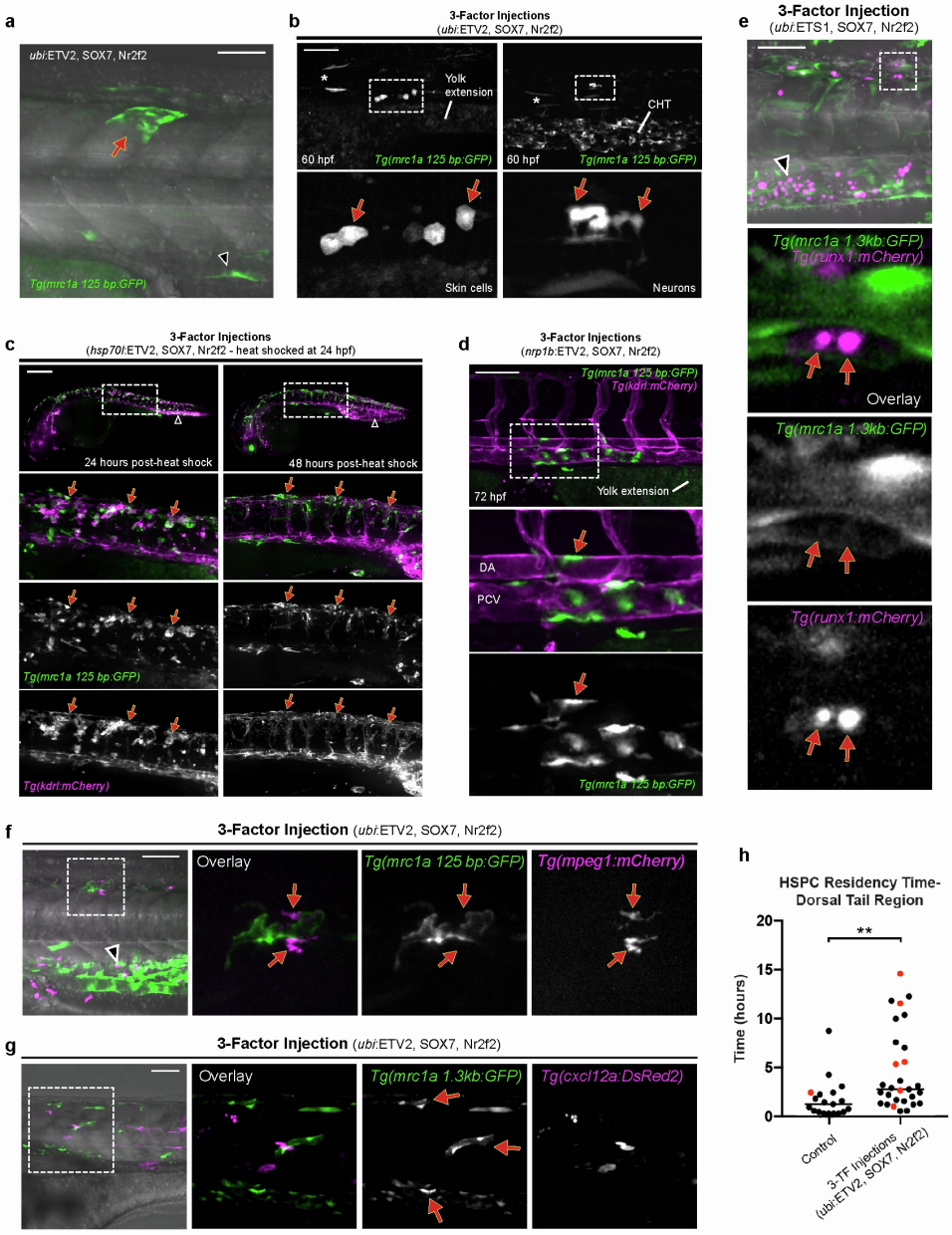

Supplemental Figure 5

Supplemental Figure 5 | Tissue-specific induction of niche EC gene expression and ectopic recruitment of HSPCs (related to Figures 6 and 7). a, Images show a cluster of GFP$^+$ muscle-shaped cells ectopically expressing the *mrc1a 125 bp:GFP* transgene in a *ubi*:ETV2, SOX7, Nr2f2 injected embryo. Image corresponds to Supplementary Video 4. **b**, Images show GFP$^+$ skin cells (left) and neurons (right) ectopically expressing the *mrc1a 125 bp:GFP* transgene in a *ubi*:ETV2, SOX7, Nr2f2 injected embryo. Asterisks denote expression in muscle cells. **c**, Images show ectopic expression in *mrc1a 125bp:GFP; kdrl:mCherry* double positive embryos that were injected with *hsp70l:*ETV2, SOX7, Nr2f2 plasmids at the one-cell stage and then heat shocked at 24 hpf. Magnification of boxed regions is shown at bottom. **d**, Images show ectopic expression in a *mrc1a 125bp:GFP; kdrl:mCherry* double positive embryo that was injected with endothelial-specific *nrp1b:*ETV2, SOX7, Nr2f2. Red arrow points to GFP expression in an arterial EC. Dorsal aorta (DA); posterior cardinal vein (PCV). **e**, Image shows *runx1:mCherry*$^+$ HSPCs localized outside the CHT within a dorsal ectopic region of *mrc1a 1.3kb:GFP* expression in an embryo injected with a pool of *ubi:*ETS1, SOX7 and Nr2f2. Magnifications of boxed region are shown. Red arrows point to ectopic expression or localization while black arrowheads point to normal expression or localization in this and other panels in this figure. Scale bars represent 100 μm. **f**, Images show ECs ectopically expressing *mrc1a 125bp:GFP* (boxed region) that are associated with *mpeg1:mCherry*$^+$ macrophages (red arrows), similar to ECs in the CHT (arrowhead). This data corresponds to Supplementary Video 7. **g**, Images show ECs (red arrows) in an anterior region of an embryo ectopically expressing *mrc1a 125bp:GFP* that are not associated with *cxcl12a:DsRed2*$^+$ stromal cells. **h**, Graph reports lifetime

measurements of HSPC residency outside of the CHT in control and 3-factor injected embryos. Red dots correspond to cells that divided. Mann-Whitney test; **P<0.01. Scale bars represent 100 μm in **a-b, d-g**. All experiments were performed at least three times, with independent clutches.

Supplementary Table 4 | *In vivo* screening of predicted enhancer elements (related to Figure 3)

Type of Element	Gene Name	Genomic Coordinates of ATAC-seq Element[a]	Relative to TSS (kb)	Amplicon Size (bp)	Showed Predicted GFP Expression Pattern[b]	Element Contains Ets, SoxF and NHR Motifs
CHT EC Element	*ap1b1*	chr5:26463217-26463695	17	750	Yes	Yes
	cltca	chr10:29,047,274-29,047,619	2.8	404	Yes	Yes
	dab2	chr5:33,980,000-33,980,306	-3.5	394	Yes	Yes
	exoc3l2a	chr5:38359097-38359903	5.9	901	Yes	Yes
	glula	chr2:19,458,704-19,459,047	4.8	446	No	Yes
	gpr182	chr23:36701205-36701682	-4.9	481	Yes	Yes
	gpr182	chr23:36694073-36694476	-2.8	398	Yes	Yes
	gpr182	chr23:36696363-36696656	1.6	577	Yes	Yes
	lgmn	chr13:36,448,465-36,448,818	2.9	414	Yes	Yes
	prcp	chr15:10,400,588-10,400,868	23	334	No	No[c]
	sele	chr20:34,010,027-34,010,326	-9.7	398	Yes	Yes
	sele	chr20:34,011,251-34,011,563	-8.5	360	Yes	Yes
	snx8a	chr3:42,090,805-42,091,062	5.5	395	No	Yes
	stab1	chr22:10467346-10467937	-2.8	874	Yes	Yes
	stab2	chr4:9790795-9791116	4.3	422	Yes	Yes
Pan-EC Element	*cdh5*	chr7:45457842-45458791	13	823	Yes	Yes
	clec14a	chr17:10362325-10362844	-3.1	455	Yes	Yes
	dll4	chr20:28219013-28219619	-55	452	Yes	No[c]
	fli1a	chr18:47039842-47040466	47	800	Yes	No[c]
	lmo2	chr18:36722030-36722527	-3.6	367	Yes	No[c]
	nrp1b	chr2:43535098-43535801	-34	552	Yes	Yes

Table shows CHT EC-specific and pan-EC ATAC-seq elements that were fused to a minimal promoter and GFP and injected into one cell-stage zebrafish embryos. [a]Coordinates of MACS2 peak. [b]Expressed in CHT ECs for CHT EC elements and in vessels throughout the embryo for pan-EC elements. [c]Lacks NHR motif.

Supplementary Table 6 | Transcription factor expression in CHT ECs (related to Figure 5)

Transcription Factor	Family	FPKM	Associated with CHT EC ATAC-seq Element Containing Ets, Sox and NHR Sites*	Genomic Coordinates of Representative Element
fli1a	Ets	480.4	Yes	chr18:46966409-46966698
etv2	Ets	192.3	Yes	chr16:44782409-44782895
ets1	Ets	183	Yes	chr18:46883643-46884100
sox18	SoxF	206.4	Yes	chr23:8886011-8886744
sox7	SoxF	125.1	Yes	chr20:19158376-19158663
nr2f2	NHR	84.6	Yes	chr18:23728906-23729747
rxraa	NHR	45.9	Yes	chr21:16411020-16411531

Table shows FPKM expression values in CHT ECs for highly expressed members of the Ets, Sox and NHR transcription factor families.
*Within 100 kb of TSS; some genes are associated with multiple elements.

Supplementary Table 7 | Transcription factor expression in mouse hematopoietic niche (related to Figure 5)

Transcription Factor	Family	Mouse E14-E15 Liver EC FPKM	Mouse E16-E17 Liver EC FPKM	Mouse Adult Bone Marrow EC FPKM
Ets1	Ets	218.4666	251.9493	153.2657
Erg	Ets	46.64156	78.53131	45.14673
Elk4	Ets	9.369453	11.4226	22.83457
Elk1	Ets	7.003965	9.08418	6.8779
Etv1	Ets	2.203135	3.10327	1.488542
Etv2	Ets	0.235977	0	0
Sox18	SoxF	127.1509	262.44	130.1783
Sox7	SoxF	49.94503	46.9365	19.80563
Sox17	SoxF	33.01219	68.37438	90.24645
Sox11	SoxF	12.01665	11.1584	0.67509
Sox12	SoxF	11.81507	21.5267	0.556478
Sox6	SoxF	1.741399	1.158524	0.51182
Sox5	SoxF	0.193041	0.289841	0.437005
Sox9	SoxF	0.119527	0.072563	0
Nr2f2	NHR	58.97832	103.5558	63.17458
Rxra	NHR	23.98264	33.0942	22.08392
Rara	NHR	19.29841	27.37294	13.93433
Nr4a2	NHR	10.13413	3.130986	30.30394
Esrrb	NHR	6.219864	7.884516	0.586381
Rora	NHR	1.219604	1.086872	5.922048

Supplementary Table 9 | Primers used to clone promoter and enhancer elements (related to Figure 3)

Type of Element	Gene	Genomic Coordinates of ATAC-seq Element	Amplicon Size (bp)	Forward	Reverse
5' upstream of TSS	*mrc1a* (1.3 kb)	chr7:65,468,213-65,469,565	1353	CTTTTGGCCATTACTGCCG	TTCTGTCTTTTAATCAGCAATCC
CHT EC element	*mrc1a* (125 bp)	chr7:65469086-65469210	125	GCTCTCAGTTCCTGGTATTTTTCT	TGAAGCTTGTACCTTTCATTTCC
5' upstream of TSS	*sele* (5.3 kb)	chr20:34,001,481-34.006.781	5301	TCGTTACTGCACTTGAAAGCGT	TATCAGTGATGTTCTGCAGTGGTC
CHT EC element	*sele* (158 bp)	chr20:34004805-34004962	158	CCATGAAACTGGGAAGATGAA	CAGGAAGAAATAATGGCAAAAA
CHT EC element	*ap1b1*	chr5:26463217-26463695	750	GAAGCTCTCCAGCAGCTCA	CATTTCCACCAGCTGTCTGAT
CHT EC element	*cltca*	chr10:29,047,274-29.047.619	404	GCTGTCAGCACATTCTTTTCC	CCCTGCTGATCACACATGAC
CHT EC element	*dab2*	chr5:33,980,000-33,980,306	394	ACTGCTCCTCACCAATCGTC	TGCACTAAATCTGTGCCAAGTC
CHT EC element	*exoc3l2a*	chr5:38359097-38359903	901	TTTATATAATCGGAAGGAACCTTTTT	TCCTGTCAGCTGTTTTCATCC
CHT EC element	*glula*	chr2:19,458,704-19,459,047	446	GGCAAAATGCTTAGATGCAGA	TGCGAGGAGGACATAAACAA
CHT EC element	*gpr182*	chr23:36701205-36701682	481	TAGCCTTGTGCAATGCTTGT	TGCTGAATTCAAAAGCCACTT
CHT EC element	*gpr182*	chr23:36694073-36694476	398	CACTTCTGGTACCAAATGATCAAC	GAGGGTTAAACGTGGCCTTA
CHT EC element	*gpr182*	chr23:36696363-36696656	577	GCGGCAAACTTTTTGAGTGT	GCCAGCCTCAAAGTTTGTTCT
CHT EC element	*lgmn*	chr13:36,448,465-36,448,818	414	CGCGTGATGAGGATCTGATT	GGTGTTGAAAGGTGATGCTG
CHT EC element	*prcp*	chr15:10,400,588-10,400,868	334	AAAATTAAGAGCGGGCAGACT	TGGAAACAACAACAGCCTGA
CHT EC element	*sele*	chr20:34,010,027-34,010,326	398	AAAGCACTTGATTGAGAATTGC	TGTTTGGTTCAGTTACACGTTTT
CHT EC element	*sele*	chr20:34,011,251-34,011,563	360	CAGTTTCCCAAGCTTCAAGG	TGTGATTACACATTCCCACACAT
CHT EC element	*snx8a*	chr3:42,090,805-42,091,062	395	AATGGTTGCAGCATTGTGTT	GCTTTTGTTTGGTGATGTGC
CHT EC element	*stab1*	chr22:10467346-10467937	874	GTTACCTGGCAACCACCAAC	TGGTCAGAATAAGCACGTTTCA
CHT EC element	*stab2*	chr4:9790795-9791116	422	ACGTTAACAAAGGCGATGTTTT	TCTAAACAATTTTTAAGGTAAACCAAA
Pan-EC element	*cdh5*	chr7:45457842-45458791	823	TGACAGGACTCATCAGCACG	AATAGTCTCTGGTCTGCTGTTAAA
Pan-EC element	*clec14a*	chr17:10362325-10362844	455	TGGGAAAAATACCAGGAAGCGT	AAGCAGCGAGCTCTCATAATAAA
Pan-EC element	*dll4*	chr20:28219013-28219619	452	AGATCAATGAGAGCGAGGCG	GGAGCAGATGAGGTTAAGTCCT
Pan-EC element	*fli1a*	chr18:47039842-47040466	800	CGGACAGTAATGTCTGGATGG	CCACAACTCCATACTGGGAAA
Pan-EC element	*lmo2*	chr18:36722030-36722527	367	TCATCATGGCCAACAGAATG	GTGCAGGAAATGAGCACAGA
Pan-EC element	*nrp1b*	chr2:43535098-43535801	552	TGACTCAACCAATCAATCAGCCT	TAGCAAAGCTCTCAGGCCC

Supplementary Table 10 | Sequences and primers for mutational variants of the 125 bp *mrc1a* and 158 bp *sele* enhancer elements (related to Figure 4)

Gene	Fragment Name	Total Fragment Sequence	Forward Primer	Reverse Primer
mrc1a	Wild-type	CCATGAAACTGGGAAGATGAAAGCATTAG TTGAATTGTTACTGGCAACATCTTCTCTGT AATGCCCCCTGTGACCCATATTGTCTCGCT CTTTCCTTTATAAACAGAGCTGTAGATATC CACAGGAAATGGGGGTGTTTTTGCCATTA TTTCTTCCTG	TGAAGCTTGTACCTTTCATTTCCTTTTTGC TGAGCTTTATTTTCTCTAGAATTGCCATTG TGTTTCCATTCTAG	GCTCTCAGTTCCTGGTATTTTTCTTTCAGC TGAAAAAAAAAATGCTGATTTGCTAGAATGG AAACACAATGGCAAT
mrc1a	Ets mutant	TGAAGCTTGTACCTTTCATTTaaaTTTTGCT GAGCTTTATTTTCTCTAGAATTGCCATTGT GTTTCCATTCTAGCAAATCAGCATTTTTTTT TCAGCTGAAAGAAAAATACCAtttACTGAGA GC	TGAAGCTTGTACCTTTCATTTaaaTTTTGCT GAGCTTTATTTTCTCTAGAATTGCCATTGT GTTTCCATTCTAG	GCTCTCAGTaaaTGGTATTTTTCTTTCAGCT GAAAAAAAAATGCTGATTTGCTAGAATGGA AACACAATGGCAAT
mrc1a	Sox mutant	TGAAGCTTGTACCTTTCATTTCCTTTTTGC TGAGCgggcggggaTCTAGAATTGCacggtgGTT TCCATTCTAGCAAATCAGCcgggggTTTCAG CTGAAAGAAAAATACCAGGAACTGAGAGC	TGAAGCTTGTACCTTTCATTTCCTTTTTGC TGAGCgggcggggaTCTAGAATTGCacggtgGTT TCCATTCTAG	GCTCTCAGTTCCTGGTATTTTTCTTTCAGC TGAAAccccccgGCTGATTTGCTAGAATGGA AACcaccgtGCAAT
mrc1a	NHR mutant	attAGCagatTtaaTTTCATTTCCTTTTTGCattaa TTTATTTTCTCTAGAATTGCCATTGTGTTT CCATTCTAGCAAATCAGCATTTTTTTTTCAG CTGAAAGAAAAATACCAGGAACTGAGAGC	attAGCagatTtaaTTTCATTTCCTTTTTGCattaa TTTATTTTCTCTAGAATTGCCATTGTGTTT CCATTCTA	GCTCTCAGTTCCTGGTATTTTTCTTTCAGC TGAAAAAAAAATGCTGATTTGCTAGAATGG AAACACAATGGCAAT
mrc1a	Control mutant	TGAAGCTTGTACCTTTCATTTCCTTTTTGC TGAGCTTTATTTTCTCTAGAATTGCCATTG TGTTTCCATTCcgGCAAATCAGCATTTTTTT TTCAGCTGAccGAAAAATACCAGGAACTGA GAGC	TGAAGCTTGTACCTTTCATTTCCTTTTTGC TGAGCTTTATTTTCTCTAGAATTGCCATTG TGTTTCCATTCTAG	GCTCTCAGTTCCTGGTATTTTTCggTCAGCT GAAAAAAAAATGCTGATTTGCcgGAATGGA AACACAATGGCAAT
sele	Wild-type	CCATGAAACTGGGAAGATGAAAGCATTAG TTGAATTGTTACTGGCAACATCTTCTCTGT AATGCCCCCTGTGACCCATATTGTCTCGCT CTTTCCTTTATAAACAGAGCTGTAGATATC CACAGGAAATGGGGGTGTTTTTGCCATTA TTTCTTCCTG	CCATGAAACTGGGAAGATGAAAGCATTAG TTGAATTGTTACTGGCAACATCTTCTCTGT AATGCCCCCTGTGACCCATATTGTCTCGCT CT	CAGGAAGAAATAATGGCAAAAACACCCCCA TTTCCTGTGGATATCTACAGCTCTGTTTAT AAAGGAAAGAGCGAGACAATATGGGTCAC AG
sele	Ets mutant	CCATGAAACTGGGAAGATGAAAGCATTAG TTGAATTGTTACTGGCAACATCTTCTCTGT AATGCCCCCTGTGACCCATATTGTCTCGCT CTTTaaaTTATAAACAGAGCTGTAGATATCC ACAtttAATGGGGGTGTTTTTGCCATTATTT CTaaaTG	CCATGAAACTGGGAAGATGAAAGCATTAG TTGAATTGTTACTGGCAACATCTTCTCTGT AATGCCCCCTGTGACCCATATTGTCTCGCT CT	CAtttAGAAATAATGGCAAAAACACCCCCATT aaaTGTGGATATCTACAGCTCTGTTTATAAtt tAAAGAGCGAGACAATATGGGTCACAG
sele	Sox mutant	CCATGAAACTGGGAAGATGAAAGCATTAG TTGAAggtggACTGGCAACATCTTCTCTGTAA TGCCCCCTGTGACCCATAggtgaTCGCTCTTT CCTTTATAAACAGAGCTGTAGATATCCACA GGAAATGGGGGTGTTTTTGCCATTATTTC TTCCTG	CCATGAAACTGGGAAGATGAAAGCATTAG TTGAAggtggACTGGCAACATCTTCTCTGTAA TGCCCCCTGTGACCCATAggtgaTCGCTCT	CAGGAAGtttattaGGCAAAAACACCCCCATTT CCTGTGGATATCTACAGCTCTGTTTATAAAA GGAAAGAGCGAtcaccTATGGGTCACAG
sele	NHR mutant	CCATGAAACTGGGAAGATGAAAGCATTAG TTGAATTGTTACTGGCAACATCTTCTCTGT AATGCCCCCTGattaaCATATTGTCTCGCTCT TTCCTTTATAAACAGAGCTGTAGATATCCA CAGGAAATGGGGGTGTTTTTGCCATTATT TCTTCCTG	CCATGAAACTGGGAAGATGAAAGCATTAG TTGAATTGTTACTGGCAACATCTTCTCTGT AATGCCCCCTGattaaCATATTGTCTCGCTCT	CAGGAAGAAATAATGGCAAAAACACCCCCA TTTCCTGTGGATATCTACAGCTCTGTTTAT AAAGGAAAGAGCGAGACAATATGttaatCAG
sele	Control mutant	CCATGAAACTGGGAAtcTGAAAGCATTAGT TGAATTGTTACTGGCAACATCTTCTCTGTA ATGCCCCCTGTGACCCATATTGTCTCGCTC TTTCCTTTATAAACAGAGagGTAGATATCCA CAGGAAATGGGGGacTTTTTGCCATTATTT CTTCCTG	CCATGAAACTGGGAAtcTGAAAGCATTAGT TGAATTGTTACTGGCAACATCTTCTCTGTA ATGCCCCCTGTGACCCATATTGTCTCGCTC T	CAGGAAGAAATAATGGCAAAAAgtCCCCCAT TTCCTGTGGATATCTAcctCTCTGTTTATAA AGGAAAGAGCGAGACAATATGGGTCACAG

Lowercase letters indicate base pair changes used to disrupt transcription factor binding motifs.

Supplementary Table 11 | Primers used for cloning and EMSA probe synthesis (related to Figure 4)

Category	Primer Name	Forward	Reverse	Comment
Cloning	*Nr2f2*	CGGGATCCatggca atggtagtca gcacg	CCGGAATTCCGGttgaattgccatatatggc	
Probe synthesis	*mrc1a* site 1 wild-type	tttaTGAAGCTTGTACCTTTCATTTCCTTTTTG	CAAAAAGGAAATGAAAGGTACAAGCTTCAtaaa	
Probe synthesis	*mrc1a* site 1 mutation	TTTAattAGCagatTtaaTTTCATTTCCTTTTTG	CAAAAAGGAAATGAAAttaAatctGCTaatTAAA	1st NHR site mutated like *in vivo* GFP reporter experiment
Probe synthesis	*mrc1a* site 2 wild-type	TTCATTTCCTTTTTGCTGAGCTTTATTTTC	GAAAATAAAGCTCAGCAAAAAGGAAATGAA	
Probe synthesis	*mrc1a* site 2 mutation	TTCATTTCCTTTTTGCattaaTTTATTTTC	GAAAATAAAttaatGCAAAAAGGAAATGAA	2nd NHR site mutated like *in vivo* GFP reporter experiment
Probe synthesis	*sele* wild-type	GTAATGCCCCCTGTGACCCATATTGTCTCGCTCTTTCCTTTATA	TATAAAGGAAAGAGCGAGACAATATGGGTCACAGGGGGCATTAC	
Probe synthesis	*sele* mutation	GTAATGCCCCCTGattaaCATATTGTCTCGCTCTTTCCTTTATA	TATAAAGGAAAGAGCGAGACAATATGttaatCAGGGGGCATTAC	NHR site mutated like *in vivo* GFP reporter experiment

Table shows primers used for cloning mouse *Nr2f2* into the pGEX2TK vector and DNA probes from the zebrafish *mrc1a* and *sele* enhancers.